Independent nucleon-pair motion and homologous structure in nuclei with $A \sim 150$

Chang-hua Zhang,[1] Shun-jin Wang,[1,2] and Jin-nan Gu[3]
[1]*Department of Modern Physics, Lanzhou University, Lanzhou, 730000, People's Republic of China*
[2]*Institute of Modern Physics, Southwest Jiaotong University, Chengdu, 610031, People's Republic of China*
[3]*Institute of Modern Physics, Academia Sinica, Lanzhou, 730000, People's Republic of China*
(Received 29 December 1997)

Shell model calculations are carried out for nuclei with $148 \leqslant A \leqslant 152$ assuming $^{146}_{64}Gd_{82}$ as an inert core. A weak coupling scheme is used to analyze the experimental data and the calculated results. The essential role of the proton intruder state $\pi h_{11/2}$, the large energy gaps between the neutron single-particle states $\nu f_{7/2}$ and the others, and the weak proton-neutron interaction provide a simple and interesting picture for the spectra and wave functions, i.e., the independent nucleon-pair motion and the corresponding homologous structure. The proton pairs in $\pi h_{11/2}$, $\pi d_{3/2}$, and $\pi s_{1/2}$ orbitals and the neutron pair in $\nu f_{7/2}$ or $\nu f_{7/2} h_{9/2}$ orbitals in nuclei $^{150,152}_{68}Er_{82,84}$ and $^{150}_{66}Dy_{84}$ are moving almost independently in the mean field provided by the core. Therefore, the yrast states below 5.3 MeV of these nuclei can be finely explained as the compositions of the excitations of these independent nucleon pairs. The negative parity levels of nuclei $^{149}_{66}Dy_{83}$, $^{149}_{65}Tb_{84}$, $^{151}_{67}Ho_{84}$, and $^{153}_{69}Tm_{84}$ can be well interpreted in terms of the concept of homologous states, i.e., the level structures in nuclei $^{149}_{66}Dy_{83}$, $^{149}_{65}Tb_{84}$, $^{151}_{67}Ho_{84}$, and $^{153}_{69}Tm_{84}$ are homologous to those of the parent structure in nuclei $^{148}_{66}Dy_{82}$, $^{148}_{64}Gd_{84}$, $^{150}_{66}Dy_{84}$, and $^{152}_{68}Er_{84}$, respectively. The level structure of the nucleus $^{151}_{68}Er_{83}$, homologous to that of parent states in the nucleus $^{150}_{68}Er_{82}$, is predicted and quite impressive in our full shell model calculation. This desires experiments to verify. The conditions for the onset of the independent nucleon-pair motion and the homologous structure are discussed in detail. [S0556-2813(98)00207-6]

PACS number(s): 21.60.Cs, 21.10.Hw, 21.10.Jx, 27.70.+q

I. INTRODUCTION

The structures of nuclei in $A \sim 150$ mass region have attracted a great deal of attention because $^{146}_{64}Gd_{82}$ can be treated as an inert core and many properties of the nuclei in this mass region can be well described in the framework of the spherical shell model [1–3]. For example, the spectra of the nuclei with proton number $Z = 64 + z$ and neutron number $N = 82$ can be well described by the $\pi h^z_{11/2}$ configuration using the empirical two-body matrix elements extracted from the spectrum of $^{148}_{66}Dy_{82}$ [1,4,5]. Some simple shell model calculations were carried out to explain the levels. Horn *et al.* [6] carried out calculations of the high-spin states of Dysprosium isotopes with up to four valence nucleons. Zhang *et al.* [7] calculated the high-spin states of the nuclei with $N = 84$ using the configurations $\pi h^z_{11/2} \nu f^2_{7/2}$ and $\pi h^z_{11/2} \nu f_{7/2} h_{9/2}$, and the agreement with experiments is very satisfactory. However, up to now, no systematic shell model calculation in a unified model space has been performed, especially for the nuclei having both valence protons and neutrons. Simple shell model calculations are inadequate for some cases where the neglected proton and neutron single-particle states $\pi d_{3/2}$, $\pi s_{1/2}$, $\nu p_{3/2}$, $\nu f_{5/2}$, etc. have important contributions. Moreover, the most important thing which has not been discussed in references is that a lot of spectra in this mass region can be well explained by a weak coupling scheme. That is, we can decompose the potential part of the Hamiltonian as

$$V = V_p + V_n + V_{pn}, \tag{1}$$

where V_p, V_n, and V_{pn} are proton-proton, neutron-neutron, and proton-neutron interactions, respectively. Since the valence protons and neutrons are distributed in two different major shells, the average interaction $\overline{V_{pn}}$ is much weaker than those of $\overline{V_p}$ and $\overline{V_n}$. Therefore, the Hamiltonian can be diagonalized using the following bases [8]:

$$\Psi_{IM} = [\phi^p_{J_1\alpha} \times \psi^n_{J_2\beta}]_{IM}, \tag{2}$$

where

$$H_p \phi^p_{J_1\alpha} = E^p_{J_1\alpha} \phi^p_{J_1\alpha}, \tag{3}$$

$$H_n \psi^n_{J_2\beta} = E^n_{J_2\beta} \psi^n_{J_2\beta}, \tag{4}$$

with $J_1\alpha$ and $J_2\beta$ as two complete sets of quantum numbers needed to label the corresponding eigenstates. In order to diagonalize the Hamiltonian, one should, in principle, include all the eigenbases of Eq. (2) in the model space. In our cases, as will be shown, the intruder proton single-particle state $\pi h_{11/2}$, the large energy gaps between neutron single-particle states $f_{7/2}$, and the others in the $^{147}_{64}Gd_{83}$, and the above mentioned weak V_{pn} interaction play an essential role in the weak coupling scheme and provide us a simple picture for analyzing the results of our full shell model calculations. For example, the spectrum of $^{150}_{66}Dy_{84}$ can be well understood in terms of compositions of the independent excitations of the proton pair in the $\pi h_{11/2}$ orbital and the neutron pair in the $\nu f_{7/2}$ orbital. We call this phenomenon independent nucleon-pair motion. Another example is the spectrum of $^{149}_{66}Dy_{83}$, which can be understood as weakly coupling a $\nu f_{7/2}$ neutron to the proton pair states $\pi h^2_{11/2}$. This weak coupling leads to the structure of the spectrum very similar to that of $^{148}_{66}Dy_{82}$. We call this similarity homologous struc-

ture. The above pictures of the independent nucleon-pair motion and the homologous state structure indicate that the spectra can be well reproduced by selecting a few physically relevant bases from Eq. (2) to diagonalize the total Hamiltonian. Similar phenomena happen in $A\sim 90$ and 208 mass regions [9–12] and the concept of homologous states has been successfully used in analysis in these cases [12].

In this paper, the details of the spectra, both the low-lying states and the high-spin high-lying states of the nuclei with proton number $Z=64+z$ and neutron number $N=82+n$ are calculated in a single shell model space using the same residual interactions. The purpose of this work is to show the existence of the independent nucleon-pair motion and the corresponding homologous state structure in this mass region. The paper is organized as follows. In Sec. II we discuss how the shell model space and the residual interactions are constructed. The analyses of the spectra and the calculated wave functions are presented in Sec. III where we show the phenomena of the independent nucleon-pair motion and the corresponding homologous state structure, and the conditions for them to appear. Discussions and conclusions are given in Sec. IV. All the calculations are carried out using the shell model code OXBASH [13].

II. MODEL SPACE AND EFFECTIVE INTERACTIONS

Because of computational difficulties, it is impossible to treat the valence nucleons in the full $Z=50\sim 82$ proton major shell and the full $N=82\sim 126$ neutron major shell. One should desire truncated calculations for these nuclei. It is well known that the nucleus $^{146}_{64}\mathrm{Gd}_{82}$ can be treated as a quasidoubly closed nucleus [1–3]. There is evidence that a number of properties of the nuclei with $N=82$ and above $^{146}_{64}\mathrm{Gd}_{82}$ can be described by the configuration of filling $Z-64$ valence protons in the intruder single-particle state $\pi h_{11/2}$. For example, the $N=82$, $0^+\rightarrow N=83$, 1^+ Gamow-Teller transition strength ratios $B_{\mathrm{GT}}(\mathrm{Dy}\rightarrow\mathrm{Tb}):B_{\mathrm{GT}}$ (Er $\rightarrow$Ho):B_{GT} (Yb$\rightarrow$Tm)$\approx$1:2:3 [14]. This evidence can greatly reduce the model space in a reasonable way. In this truncated scheme the single-particle states for valence protons are $\pi 2d_{3/2}$, $\pi 3s_{1/2}$, and $\pi 1h_{11/2}$. For the valence neutrons, we adopt two model spaces: for the first one we only select $\nu 2f_{7/2}$ and $\nu 1h_{9/2}$ single-particle states; for the other one we include all the neutron single-particle states in the $82\sim 126$ major shell. The single-particle energies of protons are extracted from the differences between the binding energies of the single-particle excited states of $^{147}_{65}\mathrm{Tb}_{82}$ and that of the ground state of $^{146}_{64}\mathrm{Gd}_{82}$ [14]. The neutron single-particle states $\nu 2f_{7/2}$, $\nu 3p_{3/2}$, $\nu 1h_{9/2}$, and $\nu 3p_{1/2}$ above $N=82$ are identified from the nucleus $^{147}_{64}\mathrm{Gd}_{82}$ [15] and their single-particle energies are extracted from the experimental data. The remaining $\nu 2f_{5/2}$ and $\nu 1i_{13/2}$ are not observed and the estimated single-particle excitation energies of 2.0 [3] and 2.5 MeV are used for the two states. The excitation energy we adopt here for the single-particle state $\nu 1i_{13/2}$ is about 0.4 MeV higher than that used in Ref. [3]. The reasons will be given in the next section.

In this mass region no definite residual interactions are available. Thus the ROT interaction in OXBASH [13] is truncated according to our first model space and denoted as ROT64. For our second model space, the Schiffer-True (ST2) [16] potential is used to generate all the two body matrix elements (TBMEs) using the harmonic oscillator wave functions with $\hbar\omega=7.644$ MeV ($\hbar\omega=41A_c^{-1/3}-25A_c^{-2/3}$ and $A_c=146$) and denoted as ST64. In the calculation, we found that the proton-neutron TBMEs and the neutron-neutron TBMEs should be scaled by factors of 0.60 and 0.8, respectively, in order to reproduce the binding energies and improve the calculated spectra of $^{148}_{65}\mathrm{Tb}_{83}$ and

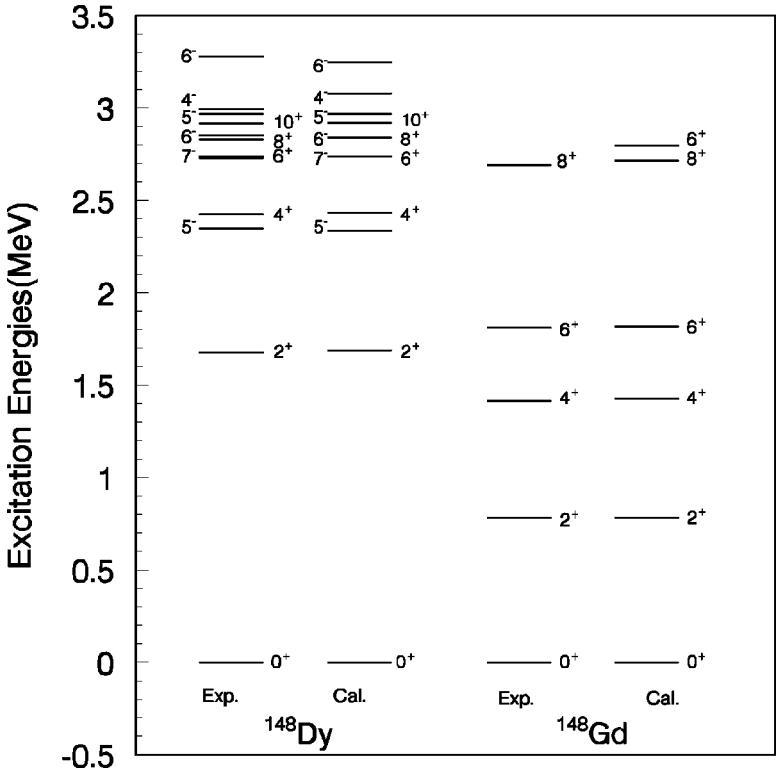

FIG. 1. The experimental and best fitted energy levels of $^{148}_{66}\mathrm{Dy}_{82}$ and $^{148}_{64}\mathrm{Gd}_{84}$. The full shell model calculation is performed using the modified ST2 [16] interactions in which some diagonal TBMEs are replaced by the scaled empirical TBMEs to include configurations mixtures (see the text).

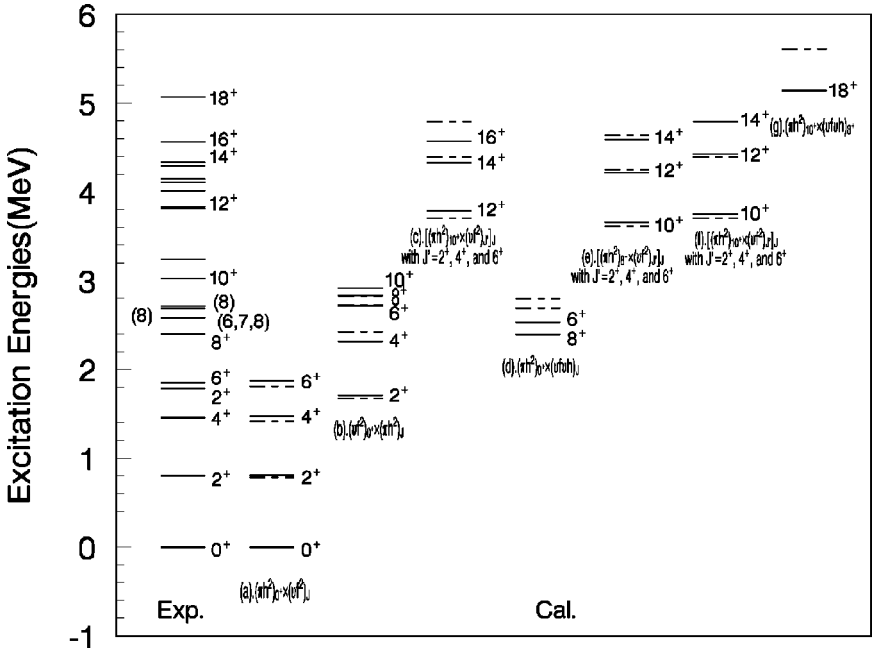

FIG. 2. The energy levels of $^{150}_{66}Dy_{84}$. The solid lines in sets (a)–(g) are the results of full shell model calculation and the dashed lines are the results of independent pair approximation, i.e., simply adding up the corresponding independent pair excitation energies $E^{p}_{J_1}$ in $^{148}_{66}Dy_{82}$ and $E^{n}_{J_2}$ in $^{148}_{64}Gd_{84}$. The prominent configurations of these levels are also displayed in each set of levels. The abbreviations $\pi h = \pi h_{11/2}$, $\nu f = \nu f_{7/2}$, and $\nu h = \nu h_{9/2}$ are used.

$^{148}_{64}Gd_{84}$. To improve the calculated results, many diagonal TBMEs generated from the scaled ST2 potential are modified according to the empirical TBMEs extracted from the spectra of $^{148}_{66}Dy_{82}$, $^{148}_{65}Tb_{83}$, and $^{148}_{64}Gd_{84}$ without configuration mixings. A factor of 0.9 is used to scale these empirical TBMEs to get a best fit of the spectra of the nuclei with $A = 148$ when configuration mixings are included. We found that the value 2.5 MeV of the excitation energy for the neutron single-particle state $\nu 1i_{13/2}$ is the best one to reproduce the binding energy of $^{148}_{64}Gd_{84}$ if the factor of 0.9 is used to scale the empirical neutron-neutron TBMEs. This finally modified ST2 interaction is denoted as ST64M.

The calculations are performed in the full ST64 model space for the nuclei with $148 \leqslant A \leqslant 152$ except $^{152}_{66}Dy_{86}$. For comparison, the calculations in the ROT64 model space are also performed for all the nuclei and the results are very similar to those of the simple shell model calculations, such as those in Ref. [7], and thus will not be presented in the paper. All the experimental data are obtained from the electronic version of the nuclear data sheets [14].

III. CALCULATED RESULTS

A. Energy levels of $^{148}_{66}Dy_{82}$ and $^{148}_{64}Gd_{84}$: Structures of proton pair and neutron pair

The experimental [14] spectra of $^{148}_{66}Dy_{82}$ and $^{148}_{64}Gd_{84}$, and their best fits are compared in Fig. 1. These two nuclei together with $^{148}_{65}Tb_{83}$ provide us with not only the information about the two-body matrix elements of the interactions in the selected model space, but also the building blocks for the spectra of nuclei with $A \sim 150$ (see below). The wave functions of the positive parity states up to 10^+ in $^{148}_{66}Dy_{82}$ consist of the configuration $\pi h^2_{11/2}$ except the 0^+ and 2^+ states which are affected by the configurations of $\pi s^2_{1/2}$, $\pi d^2_{3/2}$, and $\pi d_{3/2} s_{1/2}$. The component of the configuration $\pi h^2_{11/2}$ for the 0^+ state is acutely dependent on the pair energies in $\pi h^2_{11/2}$, $\pi d^2_{3/2}$, and $\pi s^2_{1/2}$. In our calculation, the pair energies in $\pi s^2_{1/2}$ and $\pi d^2_{3/2}$ are generated by the ST2 potential and that in $\pi h^2_{11/2}$ is obtained by scaling the empirical TBMEs extracted from the experimental spectrum of $^{148}_{66}Dy_{82}$ without configuration mixing. The same procedure is used to calculate the 2^+ state and the negative parity states if there are configuration mixings. The empirical TBMEs are used to calculate the other states which are pure stretch states constructed from the configuration $\pi h^2_{11/2}$, $\pi h_{11/2} s_{1/2}$, or $\pi h_{11/2} d_{3/2}$.

The positive parity states up to 6^+ of $^{148}_{64}Gd_{84}$ can be reproduced quite well by the configuration $\nu f^2_{7/2}$ because of the large single-particle energy gaps between $\nu f_{7/2}$ and the other neutron single-particle states. The 8^+ state is given rise from the configuration $\nu f_{7/2} h_{9/2}$ due to angular momentum requirement. This configuration also has an effect on the other states, and as neutron number increases, this effect will be amplified as a result of the reduction of the gaps between single-particle states $\nu f_{7/2}$, $\nu h_{9/2}$, etc. The spectrum is best reproduced as the factors of 0.8 and 0.9 are used to scale the TBMEs of the ST2 potential and the empirical TBMEs, respectively.

The internal excitations of the proton pair in $\pi h_{11/2}$, $\pi d_{3/2}$, and $\pi s_{1/2}$ orbitals of $^{148}_{66}Dy_{82}$, and the neutron pair in $\nu f_{7/2}$ or in $\nu f_{7/2} h_{9/2}$ orbitals of $^{148}_{64}Gd_{84}$ provide not only the good descriptions of the low-lying spectra of $^{148}_{66}Dy_{82}$ and $^{148}_{64}Gd_{84}$, but also the building blocks to establish the spectra of the other nuclei with $A \sim 150$. As will be shown, the spectra of $^{150}_{66}Dy_{84}$ and $^{150,152}_{68}Er_{82,84}$ can be understood from the weak coupling among pairs and those of $^{149}_{66}Dy_{83}$, $^{149}_{65}Tb_{84}$, $^{151}_{67}Ho_{84}$, and $^{151}_{68}Er_{83}$ can be well approximated by weakly coupling an odd nucleon to the corresponding parent nuclei. All the information about the weak coupling among nucleon pairs and between the odd nucleon and nucleon pairs shows a clear picture of independent nucleon pair motion as well as homologous state structure in the nuclei in the $A \sim 150$ mass region.

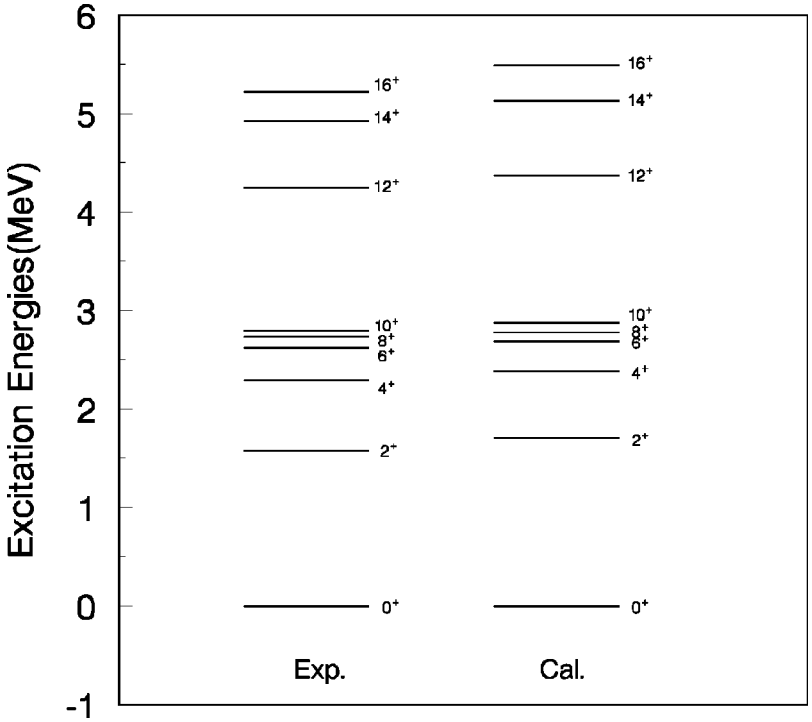

FIG. 3. The energy levels of $^{150}_{68}\mathrm{Er}_{82}$. The theoretical results are obtained from the full shell model calculation.

B. Energy levels of $^{150,152}_{66}\mathrm{Dy}_{84,86}$ and $^{150,152}_{68}\mathrm{Er}_{82,84}$

The comparisons of the experimental and calculated levels are showed in Figs. 2–5. The detailed discussions for each nucleus are as follows.

$^{150}_{66}\mathrm{Dy}_{84}$ (Fig. 2). The low-lying levels of $^{150}_{66}\mathrm{Dy}_{84}$ can be explained as a weak coupling of a proton pair excitation in the $\pi h_{11/2}$ orbital to a neutron pair excitation in the $\pi f_{7/2}$ orbital in most cases, which is clearly shown in the figure. The states up to 10^+ come from the neutron pair excitations $(\nu f^2_{7/2})_{0^+,2^+,4^+,6^+}$ and $(\nu f_{7/2}h_{9/2})_{8^+,\,6^+}$ or the proton pair excitations $(\pi h^2_{11/2})_{2^+,4^+,6^+,8^+,10^+}$, which are denoted as (a), (d), and (b), respectively. The levels of 12^+,14^+,16^+, and 18^+ which are denoted as (c) and (g), are originated from the neutron pair excitations $(\nu f^2_{7/2})_{2^+,4^+,6^+}$ and $(\nu f_{7/2}h_{9/2})_{8^+}$ based on the proton pair excitation $(\pi h^2_{11/2})_{10^+}$. The state (6,7,8) at 2.583 MeV is a possible 6^+ state from the configuration $(\pi h^2_{11/2})_{0^+}\otimes(\nu f_{7/2}h_{9/2})_{6^+}$ according to our calculation. We also show two sets of states denoted as (e) and (f) which are excited from the configurations $(\pi h^2_{11/2})_{8^+}(\nu f^2_{7/2})_{J'}$ and $(\pi h^2_{11/2})_{10^+}(\nu f^2_{7/2})_{J'}$ with $J'=2^+$, 4^+, and 6^+, respectively. Three pieces of evidence support the above assignments. One is the energy spectrum. The level spectrum of $^{150}_{66}\mathrm{Dy}_{84}$ can be approximately obtained by simply summing up the energy spectra $E^p_{J_1}$ of $^{148}_{66}\mathrm{Dy}_{82}$ and $E^n_{J_2}$ of $^{148}_{64}\mathrm{Gd}_{84}$ in a way corresponding to the above level assignment, which is shown by dashed lines in the figure. The average deviation of experimental energy levels from the independent pair approximation is less than 0.2 MeV, which implies a weak coupling between the proton pair and the neutron pair. However, larger deviations of the states 8^+, 6^+, and 18^+ in sets (d) and (g) tell that the neutron-proton interaction for $\pi h_{11/2}-\nu h_{9/2}$ is larger than that for $\pi h_{11/2}-\nu f_{7/2}$. In fact, according to our finally fitted TBMEs, the average proton-neutron interactions are about -0.301 MeV for $\pi h_{11/2}-\nu h_{9/2}$ and -0.163 MeV for $\pi h_{11/2}-\nu f_{7/2}$. This larger V_{pn} interaction for $\pi h_{11/2}-\nu h_{9/2}$ will have an important effect on the spectrum as the valence nucleon number, especially as the valence neutron number increases. The second piece of evidence is the similarity of electric quadrupole $(E2)$ transition strengths $B(E2)$. Based on the above independent nucleon-pair approximation, the $E2$ transitions of the states in sets (a) and (c) should have similar $B(E2)$ values to those of the corresponding states of $^{148}_{64}\mathrm{Gd}_{84}$. Likewise, the $E2$ transitions of the states in set (b) should have similar $B(E2)$ values to those of the corresponding states of $^{148}_{66}\mathrm{Dy}_{82}$. The calculated neutron $B(E2)$ (hereafter the effective neutron charge $e_n=0.5e$ is used) for the $E2$ transitions $16^+\rightarrow14^+\rightarrow12^+\rightarrow10^+$ in set (c) are $6.09e^2$, $9.09e^2$, and $7.35e^2$ fm^4, and they are close to the $B(E2)$ values of $4.89e^2$, $11.18e^2$, and $10.56e^2$ fm^4 for the $E2$ transitions $6^+\rightarrow4^+\rightarrow2^+\rightarrow0^+_{\mathrm{g.s.}}$ in set (a), respectively. Moreover, the calculated $B(E2)$ values for the $E2$ transitions $6^+\rightarrow4^+\rightarrow2^+\rightarrow0^+$ in $^{148}_{64}\mathrm{Gd}_{84}$ are $11.11e^2$, $26.94e^2$, and $25.73e^2$ fm^4, respectively. The calculated proton $B(E2)$ for the transitions $10^+\rightarrow8^+\rightarrow6^+\rightarrow4^+\rightarrow2^+\rightarrow0^+_{gs}$ in set (b) are $52.59e^2$, $117.1e^2$, $165.4e^2$, $161e^2$, and $102.4e^2$ fm^4, and the corresponding calculated $B(E2)$ values in the $^{148}_{66}\mathrm{Dy}_{82}$ are $51.45e^2$, $137.3e^2$, $221e^2$, $264.5e^2$, and $218.7e^2$ fm^4, respectively. The calculated $B(E2)$ of $8^+\rightarrow6^+$ in set (d) is $2.65e^2$ fm^4 and the calculated $B(E2)$ for the corresponding $8^+\rightarrow6^+$ in the $^{148}_{64}\mathrm{Gd}_{84}$ is $4.90e^2$ fm^4. The third piece of evidence comes from the calculated two-neutron and two-proton shell model spectroscopic amplitudes defined as [8,13]

$$S^{1/2}(\rho,\lambda,\Delta J\Delta T)=[(2J_f+1)(2T_f+1)]^{-1/2}\times\langle J_fT_f|||A^\dagger(\rho,\lambda,\Delta J\Delta T)|||J_iT_i\rangle, \tag{5}$$

where ρ and λ are the abbreviations of the single-particle

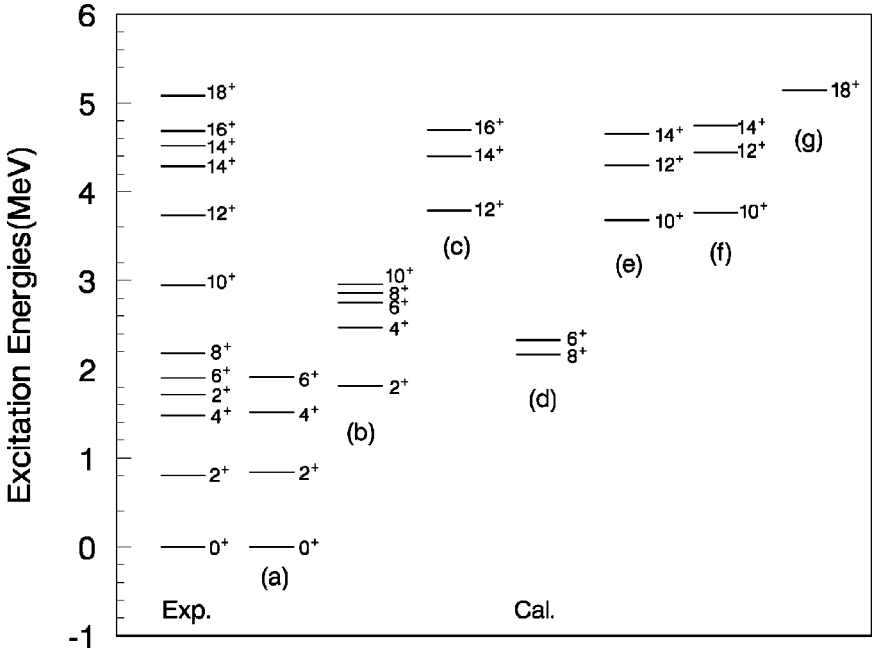

FIG. 4. The energy levels of $^{152}_{68}\mathrm{Er}_{84}$. The full shell model calculated level structures labeled by (a)–(g) and their prominent configurations are the same as those in Fig. 2.

states with quantum numbers $j_1 m_1 t_1 t_{z1}$ and $j_2 m_2 t_2 t_{z2}$, $|J_i T_i\rangle$ and $|J_f T_f\rangle$ are the initial and final state wave functions, respectively. The two-particle creation operator is defined as [8]

$$A^{\dagger}_{JMTT_z}(\rho,\lambda)=(1+\delta_{\rho\lambda})^{-1/2}\sum_{m_1 m_2 t_{z1} t_{z2}}\langle j_1 m_1 j_2 m_2|JM\rangle \times\langle t_1 t_{z1} t_2 t_{z2}|TT_z\rangle a^{\dagger}_{j_1 m_1 t_1 t_{z2}} a^{\dagger}_{j_2 m_2 t_2 t_{z2}}. \quad (6)$$

The calculated results are displayed in Tables I(a) and I(b). The two-particle shell model spectroscopic amplitudes $S^{1/2}$ $(\nu f_{7/2},\nu f_{7/2})$ for $|0^+,{}^{148}_{66}\mathrm{Dy}_{82}\rangle\rightarrow|J_f,{}^{150}_{66}\mathrm{Dy}_{84}\rangle$ and $|10^+,{}^{148}_{66}\mathrm{Dy}_{82}\rangle\rightarrow|J_f,{}^{150}_{66}\mathrm{Dy}_{84}\rangle$ are much larger than those $S^{1/2}(\pi h_{11/2},\pi h_{11/2})$ for $|0^+,{}^{148}_{64}\mathrm{Gd}_{84}\rangle\rightarrow|J_f,{}^{150}_{66}\mathrm{Dy}_{84}\rangle$ with J_f being the states in sets (a) and (c), respectively. On the other hand, the calculated two-particle shell model spectroscopic amplitudes $S^{1/2}$ $(\pi h_{11/2},\pi h_{11/2})$ for $|0^+,{}^{148}_{64}\mathrm{Gd}_{84}\rangle \rightarrow|J_f,{}^{150}_{66}\mathrm{Dy}_{84}\rangle$ are much larger than those $S^{1/2}(\nu f_{7/2},\nu f_{7/2})$ for $|0^+,{}^{148}_{66}\mathrm{Dy}_{82}\rangle\rightarrow|J_f,{}^{150}_{66}\mathrm{Dy}_{84}\rangle$ with J_f being the states in set (b). The contributions from the $\pi d_{3/2}$ or $\pi s_{1/2}$ configuration are quite small. Similar results are obtained for the states of sets (e) and (f). From the above discussion we conclude that the excitations of the proton pair in $\pi h^2_{11/2}$ and the neutron pair in $\nu f^2_{7/2}$ or $\nu f_{7/2} h_{11/2}$ are almost independent. We call this phenomenon independent nucleon pair motion in the mean field provided by the core.

$^{150}_{68}\mathrm{Er}_{82}$ (Fig. 3). The structure of positive parity states in $^{150}_{68}\mathrm{Er}_{82}$ were calculated by Lawson with a single configuration $\pi h^4_{11/2}$ using the empirical TBMEs extracted from the

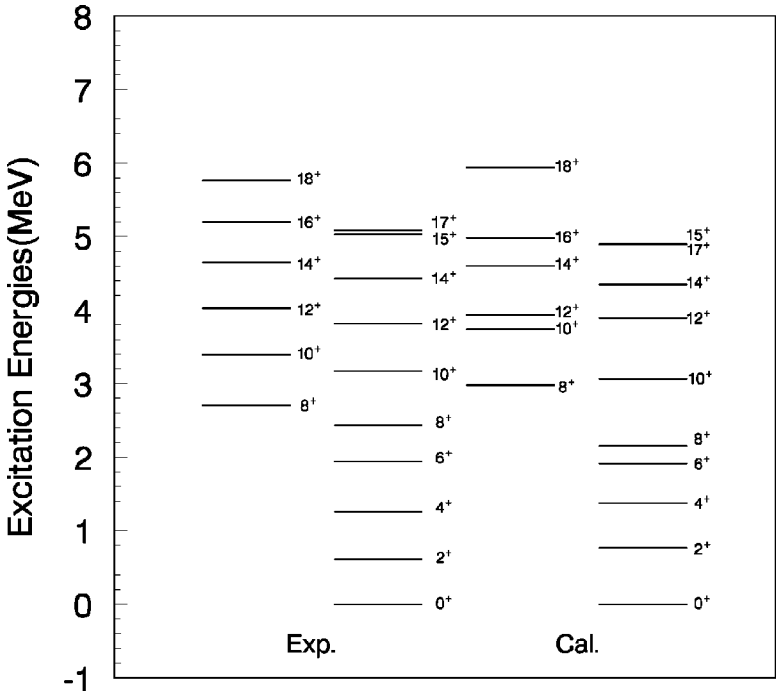

FIG. 5. Theoretical and experimental energy levels of $^{152}_{66}\mathrm{Dy}_{86}$ for the positive parity states. The two groups of levels are described in the text.

TABLE I. (a) The calculated two-neutron shell model spectroscopic amplitudes $S^{1/2}$ for the transitions $|0^+, {}^{148}_{66}\mathrm{Dy}_{82}\rangle \rightarrow |J_f, {}^{150}_{66}\mathrm{Dy}_{84}\rangle$ with J_f being the states of sets (a), (b), and (d), and the transitions $|10^+, {}^{148}_{66}\mathrm{Dy}_{82}\rangle \rightarrow |J_f, {}^{150}_{66}\mathrm{Dy}_{84}\rangle$ with J_f being the states of set (c). Here sets (a), (b), (c), and (d) are labeled in Fig. 2. (b) The two-proton shell model spectroscopic amplitudes $S^{1/2}(\pi h_{11/2}, \pi h_{11/2})$ for the transitions $|0^+, {}^{148}_{64}\mathrm{Gd}_{84}\rangle \rightarrow |J_f, {}^{150}_{66}\mathrm{Dy}_{84}\rangle$ with J_f being the states of sets (a), (b), and (d) labeled in Fig. 2.

(a)

	$J_i^\pi;T_i \rightarrow J_f^\pi;T_f$	$\Delta J;\Delta T$	E_{xf} (MeV)	ρ,λ	$S^{1/2}$
(a)	$0^+;1 \rightarrow 0^+;0$	0;1	0.000	$\nu f_{7/2}\nu f_{7/2}$	1.577
	$0^+;1 \rightarrow 2^+;0$	2;1	0.812	$\nu f_{7/2}\nu f_{7/2}$	1.634
	$0^+;1 \rightarrow 4^+;0$	4;1	1.475	$\nu f_{7/2}\nu f_{7/2}$	−1.652
	$0^+;1 \rightarrow 6^+;0$	6;1	1.872	$\nu f_{7/2}\nu f_{7/2}$	1.655
(b)	$0^+;1 \rightarrow 2^+;0$	2;1	1.710	$\nu f_{7/2}\nu f_{7/2}$	−0.416
	$0^+;1 \rightarrow 4^+;0$	4;1	2.314	$\nu f_{7/2}\nu f_{7/2}$	−0.342
	$0^+;1 \rightarrow 6^+;0$	6;1	2.710	$\nu f_{7/2}\nu h_{9/2}$	−0.151
	$0^+;1 \rightarrow 8^+;0$	8;1	2.835	$\nu f_{7/2}\nu h_{9/2}$	−0.134
(c)	$10^+;1 \rightarrow 12^+;0$	2;1	3.789	$\nu f_{7/2}\nu f_{7/2}$	−1.616
	$10^+;1 \rightarrow 14^+;0$	4;1	4.328	$\nu f_{7/2}\nu f_{7/2}$	1.524
	$10^+;1 \rightarrow 16^+;0$	6;1	4.570	$\nu f_{7/2}\nu f_{7/2}$	1.702
(d)	$0^+;1 \rightarrow 6^+;0$	6;1	2.534	$\nu f_{7/2}\nu h_{9/2}$	−1.606
	$0^+;1 \rightarrow 8^+;0$	8;1	2.395	$\nu f_{7/2}\nu h_{9/2}$	1.615

(b)

	$J_i^\pi;T_i \rightarrow J_f^\pi;T_f$	$\Delta J;\Delta T$	E_{xf} (MeV)	$S^{1/2}$
(a)	$0^+;1 \rightarrow 2^+;0$	2;1	0.812	−0.301
	$0^+;1 \rightarrow 4^+;0$	4;1	1.475	0.168
	$0^+;1 \rightarrow 6^+;0$	6;1	1.872	−0.098
(b)	$0^+;1 \rightarrow 0^+;0$	0;1	0.000	−1.564
	$0^+;1 \rightarrow 2^+;0$	2;1	1.710	−1.369
	$0^+;1 \rightarrow 4^+;0$	4;1	2.314	−1.289
	$0^+;1 \rightarrow 6^+;0$	6;1	2.710	1.471
	$0^+;1 \rightarrow 8^+;0$	8;1	2.835	1.640
	$0^+;1 \rightarrow 10^+;0$	10;1	2.918	1.638
(d)	$0^+;1 \rightarrow 6^+;0$	6;1	2.534	0.301
	$0^+;1 \rightarrow 8^+;0$	8;1	2.395	−0.120

spectrum of ${}^{148}_{66}\mathrm{Dy}_{82}$ [5]. Our full shell model calculation has some improvements. The essential new point we found here is the concept of independent motion of proton pairs. The structure of the states 0^+, 2^+, 4^+, 6^+, 8^+, and 10^+ is very similar to those in ${}^{148}_{66}\mathrm{Dy}_{82}$ and the other proton pair has small influence on these states. Thus we assign this set of states to be $(\pi h^2_{11/2})_{J^+} \otimes (\pi h^2_{11/2})_{0^+}$ with $J^+ = 0^+$, 2^+, 4^+, 6^+, 8^+, and 10^+. The 12^+, 14^+, and 16^+ states have similar energy positions as 2^+, 4^+, and 6^+ if one subtracts the excitation energy of the 10^+ state from their excited energies. So this set of states can be assigned to be $[(\pi h^2_{11/2})_{10^+} \otimes (\pi h^2_{11/2})_{2^+,4^+,6^+}]_{12^+,14^+,16^+}$. The calculated $B(E2)$'s are also close to each other for the two sets of levels. The calculated wave functions, $B(E2)$'s, and two-proton shell model spectroscopic amplitudes support the above assignments. This similarity of the level structures of the above two sets of states indicates that the interactions between proton pairs are very weak, and therefore, these proton pairs move almost independently with the restriction of Pauli's principle. The low-lying negative parity states are also reproduced in our calculations and assigned as $(\pi h^2_{11/2})^+_0 \otimes (\pi s_{1/2} h_{11/2})_{5^-,6^-}$ or $(\pi d_{3/2} h_{11/2})_{4^-,5^-,6^-,7^-}$.

TABLE II. The weights of the main configurations for the yrast states of ${}^{152}_{68}\mathrm{Er}_{84}$ up to 6^+ (in %).

Configurations	0^+	2^+	4^+	6^+
$\pi h^4_{11/2}\nu f^2_{7/2}$	58.01	63.41	66.26	65.77
$\pi d^2_{3/2} h^2_{11/2}\nu f^2_{7/2}$	15.34	19.18	17.51	16.76
$\pi s^2_{1/2} h^2_{11/2}\nu f^2_{7/2}$	7.40	8.38	8.12	7.97

${}^{152}_{68}\mathrm{Er}_{84}$ (Fig. 4). The level structure of ${}^{152}_{68}\mathrm{Er}_{84}$ is almost identical to that of ${}^{150}_{66}\mathrm{Dy}_{84}$. The dominant configurations of the states in sets (a)–(g) in the figure are similar to those in Fig. 2 of the nucleus ${}^{150}_{66}\mathrm{Dy}_{84}$. It is interesting to note that both the simple configuration shell model calculation in Ref. [7] and our full shell model calculation reproduce this identification quite well. But our calculated wave functions are quite different from those in that reference which are pure $\pi h^4_{11/2}\nu f^2_{7/2}$ or $\pi h^4_{11/2}\nu f_{7/2} h_{9/2}$. We list the wave functions in Table II for the yrast states up to 6^+ for important configurations. The most important one is the $\pi h^4_{11/2}\nu f^2_{7/2}$ configuration and the less important ones are the components of $\pi h^2_{11/2} d^2_{3/2}\nu f^2_{7/2}$ and $\pi h^2_{11/2} s^2_{1/2}\nu f^2_{7/2}$. It is interesting to note that all the wave functions listed in the table have similar configuration structures. The proton pair in $\pi d_{3/2}$ and $\pi s_{1/2}$ orbitals can at most provide two units of angular momenta. The calculated two-proton shell model spectroscopic amplitudes show that the proton pair in these two orbitals is, in most cases, in the $J=0$ state. The identification of the spectra of ${}^{150}_{66}\mathrm{Dy}_{84}$ and ${}^{152}_{68}\mathrm{Er}_{84}$ indicates that the proton-proton interactions in the $\pi h_{11/2} - \pi d_{3/2}$ and $\pi h_{11/2} - \pi s_{1/2}$ are very weak and that the proton pairs in $\pi d_{3/2}$ or $\pi s_{1/2}$ orbitals are independent of the proton pairs in the $\pi h_{11/2}$ orbital. Indeed the average interactions for $\pi h_{11/2} - \pi d_{3/2}$ and $\pi h_{11/2} - \pi s_{1/2}$ are both about 0.126 MeV calculated with ST2 potential in the ST64 model space, which are much smaller than the average interactions for $\pi h_{11/2} - \pi h_{11/2}$, $\pi d_{3/2} - \pi d_{3/2}$, and $\pi s_{1/2} - \pi s_{1/2}$. Therefore, the configurations $\pi h^2_{11/2} s^2_{1/2}\nu f^2_{7/2}$ and $\pi h^2_{11/2} d^2_{3/2}\nu f^2_{7/2}$ only slightly affect the spectrum and allow us to scale the empirical TBMEs by a factor to incorporate the configuration mixings and vice versa. After having scaled the wave functions or the TBMEs, the spectrum of ${}^{152}_{68}\mathrm{Er}_{84}$ displayed in Fig. 4 can be finely described by the configuration $\pi h^2_{11/2}\nu f^2_{7/2}$ or $\pi h^2_{11/2}\nu f_{7/2} h_{9/2}$, which is almost identical to that of ${}^{150}_{66}\mathrm{Dy}_{84}$. However, the components neglected in the simple configuration shell model calculation have important effects on other properties such as $B(E2)$ and Gamow-Teller transition strength $B(GT)$. For example, the calculated $B(GT)$ (9.96) using the simple configuration for β^+-decay ${}^{152}_{68}\mathrm{Er}_{84}(0^+) \rightarrow {}^{152}_{67}\mathrm{Ho}_{85}(1^+)$ is almost identical to that $B(GT)$ (9.66) of ${}^{150}_{68}\mathrm{Er}_{82}(0^+) \rightarrow {}^{150}_{67}\mathrm{Ho}_{83}(1^+)$. But the experimental results are

not the case. The logft for the former decay is 4.08 and that for the latter is 3.60. This indicates that the protons have some probabilities to occupy the $\pi d_{3/2}$ and $\pi s_{1/2}$ orbitals which have no contributions to the Gamow-Teller transition strengths. Therefore, the studies of the Gamow-Teller transition provide a stringent test to the shell model calculations. Our wave functions can give a more reasonable Gamow-Teller transition strength. The analyses of the Gamow-Teller transition strengths for the nuclei in this mass region will be presented elsewhere [17].

The independent nucleon-pair motion is also approximately valid for the neutron pair in the configuration $h_{9/2}f_{7/2}$ because the 8^+ and 18^+ states are approximately identical to those in $^{150}_{66}\mathrm{Dy}_{84}$. However, as neutron number increases, this is no longer true, as will be seen in $^{152}_{66}\mathrm{Dy}_{86}$ and $^{151}_{66}\mathrm{Dy}_{85}$ discussed below.

$^{152}_{66}\mathrm{Dy}_{86}$ (Fig. 5). In the calculation, we restrict the four neutrons only filling the p, f, and $h_{9/2}$ single-particle states to reduce the computational difficulty. Our calculation reproduces the correct level sequence of $^{152}_{66}\mathrm{Dy}_{86}$ up to spin 18^+ except the two levels 15^+ and 17^+. However, the independent nucleon-pair motion disappears in this nucleus. It is found from our shell model calculation that, the four valence neutrons have large occupation probabilities in the $\nu h_{9/2}$, $\nu p_{3/2,1/2}$, and $\nu f_{5/2}$ orbitals because the energy gaps between $\nu f_{7/2}$ and these neutron single-particle states have been greatly reduced due to the increase of valence neutrons. As a consequence, the independent nucleon-pair motion is destroyed and the complicated configuration distributions leads to collective properties of the spectrum in $^{152}_{66}\mathrm{Dy}_{86}$. However, the regular experimental spectrum (except 15^+ and 17^+) shows a characteristic of collective vibrations, while our calculated spectrum is less regular. This discrepancy may be related to the surface vibration in $^{152}_{66}\mathrm{Dy}_{86}$ and our shell model space is not large enough to describe it correctly.

We are now at the point where we can summarize the conditions for the onset of the independent nucleon-pair motion. First, the intruder proton state $\pi h_{11/2}$ plays an essential role for the independent nucleon-pair motion due to its high angular momentum, strong pairing energy, and negative parity in contrast to the other orbitals ($\pi s_{1/2}$ and $\pi d_{3/2}$). Moreover, the $\pi h_{11/2}$ orbital can accommodate six proton pairs, thus two proton pairs show a good independent motion. Furthermore, the proton-proton interactions in $\pi h_{11/2}-\pi d_{3/2}$ and in $\pi h_{11/2}-\pi s_{1/2}$ are quite small due to the less similarity of the relevant single-particle wave functions.

To formulate the above ideas more clearly, let us introduce the pair operators as [18]

$$\hat{\xi}_{JM}{}^{\dagger}=\frac{1}{\sqrt{2}}\sum_{m_1m_2}\langle jm_1jm_2|JM\rangle a^{\dagger}_{jm_1}a^{\dagger}_{jm_2}, \tag{7}$$

which have the following commutation relation:

$$[\hat{\xi}_0,\hat{\xi}_0^{\dagger}]=1-\frac{2\hat{N}}{2j+1}, \tag{8}$$

where $\xi_0=\xi_{J=0,M=0}$. The second term in Eq. (8) can be neglected if the particle number in the orbital is $N\ll 2j+1$. This is called the pair approximation. Under this approximation, the nucleon-pair $\hat{\xi}^{\dagger}_{JM}$ behaves as a boson. Furthermore, the weak interaction between nucleon pairs $\xi^{\dagger}_{JM}$ makes them move independently, as we have seen in the spectrum of $^{150}_{68}\mathrm{Er}_{82}$. We prefer independent pair approximation to boson approximation for two reasons: (i) the nucleon pair $\xi^{\dagger}_{JM}$ possesses fermion structure and has many internal excitations, i.e., the JM can take all allowed values, which cannot be described by a simple structureless boson. This fermion structure is fully taken into account in the shell model calculation. (ii) The commutation relation of Eq. (8) is just the kinetic condition for the independent pair approximation. The independent motion of these nucleon pairs is rooted in the weak interactions between them. This is the dynamical reason for the independent nucleon pair approximation, which is originated from the specific shell model Hamiltonian.

Under the independent nucleon-pair approximation, the ground state of $2N$ like particles in the high j orbital can be written as

$$\Psi_0(2N)=\overbrace{\hat{\xi}_0^{\dagger}\cdots\hat{\xi}_0^{\dagger}}^{N}|0\rangle \quad . \tag{9}$$

Here ξ_0 can be considered to be a ground-state pair. Because the proton-proton interactions in $\pi h_{11/2}-\pi d_{3/2}$ and $\pi h_{11/2}-\pi s_{1/2}$ are quite small and the proton pair in $\pi d_{3/2}$ and $\pi s_{1/2}$ in most cases is in the $J=0$ state, the ξ_0 can be also referred to this $J=0$ pair. The excited states can be constructed from the compositions of the weakly coupled pairs $\hat{\xi}^{\dagger}_{JM}$ such as

$$\Psi_J(2N)=[\overbrace{\hat{\xi}^{\dagger}_{J_1M_1}\cdots\hat{\xi}^{\dagger}_{J_NM_N}}^{N}]_J|0\rangle \quad . \tag{10}$$

This scheme provides a good approximation to the even-even nuclei with valence protons $z\leqslant 6$ and $N=82$. The positive parity yrast states of $^{148}_{66}\mathrm{Dy}_{82}$ can be explained as one proton pair states $\Psi_J(2)=\hat{\xi}^{\dagger}_{JM}|0\rangle$ in the $\pi h_{11/2}$ orbital with $J=0^+$, 2^+, 4^+, 6^+, 8^+, and 10^+. According to our shell model calculation, the positive parity states of $^{150}_{68}\mathrm{Er}_{82}$ can be interpreted as two proton pair states with a weak coupling, namely, $\Psi_J(4)=[\hat{\xi}^{\dagger}_{J_1M_1}\otimes\hat{\xi}^{\dagger}_{J_2M_2}]_J|0\rangle$ in the $\pi h_{11/2}$ orbital. The yrast states in $^{148}_{64}\mathrm{Gd}_{84}$ up to 6^+ can be described by one neutron pair states $\Psi_J(2)=\hat{\xi}^{\dagger}_{JM}|0\rangle$ in the $\nu f_{7/2}$ orbital. As pointed out, one of the conditions for the independent pair approximation to be valid is related to the degeneracy of the j orbital. It is expected that the goodness of this approximation is less for the neutron $f_{7/2}$ orbital. We can also extend the neutron pair states to $(\nu f_{7/2}h_{9/2})_J$ if there is only one neutron pair as we have shown in nuclei with $N=84$.

Secondly, the proton-neutron interactions in $\pi h_{11/2}-\nu f_{7/2}$ are much weaker than the like-particle pairing interactions in orbitals $\nu h_{11/2}$ and $\nu f_{7/2}$. As mentioned in Sec. I, in order to reproduce the binding energy of $^{148}_{65}\mathrm{Tb}_{83}$ using ST2 potential, one should scale the $p-n$ TBMEs by a factor of 0.6, while larger factors of 0.8 and 1.0 are needed to scale the neutron-neutron TBMEs and proton-proton TBMEs to reproduce the binding energies of $^{148}_{64}\mathrm{Gd}_{84}$ and $^{148}_{66}\mathrm{Dy}_{82}$, respectively. Thus the independent pair approximation dis-

cussed above is also valid for the nuclei which have both proton pairs and neutron pairs. Therefore, the wave functions of the ground state and excited states for even-even nuclei can be written as compositions of the proton pairs and the neutron pairs

$$\Psi_0(2N_p,2N_n)=[\overbrace{\hat{\xi}_0^{p\dagger}\cdots\hat{\xi}_0^{p\dagger}}^{N_p}]_0\otimes[\overbrace{\hat{\xi}_0^{n\dagger}\cdots\hat{\xi}_0^{n\dagger}}^{N_n}]_0|0\rangle \tag{11}$$

and

$$\Psi_J(2N_p,2N_n)=\{[\overbrace{\hat{\xi}_{J_1M_1}^{p\dagger}\cdots\hat{\xi}_{J_{N_p}M_{N_p}}^{p\dagger}}^{N_p}]_{J_p}\otimes[\overbrace{\hat{\xi}_{J_1M_1}^{n\dagger}\cdots\hat{\xi}_{J_{N_n}M_{N_n}}^{n\dagger}}^{N_n}]_{J_n}\}_J|0\rangle, \tag{12}$$

respectively, with

$$\hat{\xi}_{JM}^{p\dagger}=\frac{1}{\sqrt{2}}=\sum_{m_1m_2}\langle j^pm_1j^pm_2|JM\rangle a_{j^pm_1}^{\dagger}a_{j^pm_2}^{\dagger}, \tag{13}$$

and

$$\hat{\xi}_{JM}^{n\dagger}=\frac{1}{\sqrt{2}}\sum_{m_1m_2}\langle j^nm_1j^nm_2|JM\rangle a_{j^nm_1}^{\dagger}a_{j^nm_2}^{\dagger}, \tag{14}$$

where $j^p=\pi h_{11/2}$, $\pi d_{3/2}$ or $\pi s_{1/2}$, and $j^n=\nu f_{7/2}$ as in the definitions of $\hat{\xi}_{JM}^{p\dagger}$ and $\hat{\xi}_{JM}^{n\dagger}$. The shell model results of $^{150}_{66}\mathrm{Dy}_{84}$ and $^{152}_{68}\mathrm{Er}_{84}$ can be well classified as the composition states of one proton pair weakly coupled to one neutron pair and of two proton pairs weakly coupled to one neutron pair, respectively.

Thirdly, the large gaps between single-particle states $\nu f_{7/2}$ and $\nu h_{9/2}$, etc., play an important role in the independent nucleon-pair approximation. Unlike the $\pi h_{11/2}$ isolated from the $\pi d_{3/2}$ and $\pi s_{1/2}$, the $\nu f_{7/2}$ has the same parity and approximate angular momentum as $\nu h_{9/2}$ and $\nu f_{5/2}$. Therefore, the large energy gaps between $\nu f_{7/2}$ and $\nu h_{9/2}$ and $\nu f_{5/2}$ in $^{147}_{64}\mathrm{Gd}_{83}$ is crucial for the independent neutron-pair motion in nuclei with $N=84$. Calculations show that the independent pair picture in $^{150}_{66}\mathrm{Dy}_{84}$ is greatly destroyed as the gap between $\nu f_{7/2}$ and $\nu h_{9/2}$ is reduced from actual value 1.4 to 0.7 MeV since the neutron states can no longer be described by a single $\nu f_{7/2}$ orbital. The gaps will be reduced as neutron and proton number increase. For example, the excitation energies of the $9/2^-$ state in $^{149}_{66}\mathrm{Dy}_{83}$ and $^{151}_{64}\mathrm{Gd}_{87}$ reduce from 1.04 to 0.379 MeV. For the reasons mentioned above, the independent motion of proton pairs and neutron pairs are restricted to the nuclei with $N\leqslant 84$. We will see that it is also true for odd-even nuclei.

C. Energy levels in $^{149}_{66}\mathrm{Dy}_{83}$, $^{149}_{65}\mathrm{Tb}_{84}$, $^{151}_{67}\mathrm{Ho}_{84}$, $^{151}_{68}\mathrm{Er}_{83}$, $^{153}_{69}\mathrm{Tm}_{84}$, and $^{151}_{66}\mathrm{Dy}_{85}$

For odd-even nuclei, the ground states and excited states can be approximated as

$$\Psi_j(2N_p,2N_n,0,jm)=\{a_{jm}^{\dagger}\otimes[\overbrace{\hat{\xi}_0^{p\dagger}\cdots\hat{\xi}_0^{p\dagger}}^{N_p}]_0\otimes[\overbrace{\hat{\xi}_0^{n\dagger}\cdots\hat{\xi}_0^{n\dagger}}^{N_n}]_0\}_j|0\rangle \tag{15}$$

and

$$\Psi_J(2N_p,2N_n,J_c,j)=\{a_{jm}^{\dagger}\otimes\{[\overbrace{\hat{\xi}_{J_1M_1}^{p\dagger}\cdots\hat{\xi}_{J_NM_{N_p}}^{p\dagger}}^{N_p}]_{J_p}\otimes[\overbrace{\hat{\xi}_{J_1M_1}^{n\dagger}\cdots\hat{\xi}_{J_NM_{N_n}}^{n\dagger}}^{N_n}]_{J_n}\}_{J_c}\}_J|0\rangle, \tag{16}$$

respectively, if the independent nucleon-pair approximation holds for the even-even nucleus with $N=2N_n$ valence neutrons and $Z=2N_p$ valence protons. $a_{jm}^{\dagger}$ creates an odd neutron in the $\nu f_{7/2}$ orbital or an odd proton in the $\pi h_{11/2}$ orbital outside the even-even core. As mentioned above, the weak residual interactions lead to the spectra and wave functions of odd-even nuclei having similar structures to those of the even-even parent nuclei. This phenomenon is called homologous state structure [12]. We denote $\Psi_{J_c}(2N_p,2N_n)$ as the parent states which are excitation states of the N_p proton pairs in the $\pi h_{11/2}$ orbital and of the N_n neutron pairs in the $\nu f_{7/2}$ orbital, and $\Psi_J(2N_p,2N_n,J_c,j)$ as the homologous

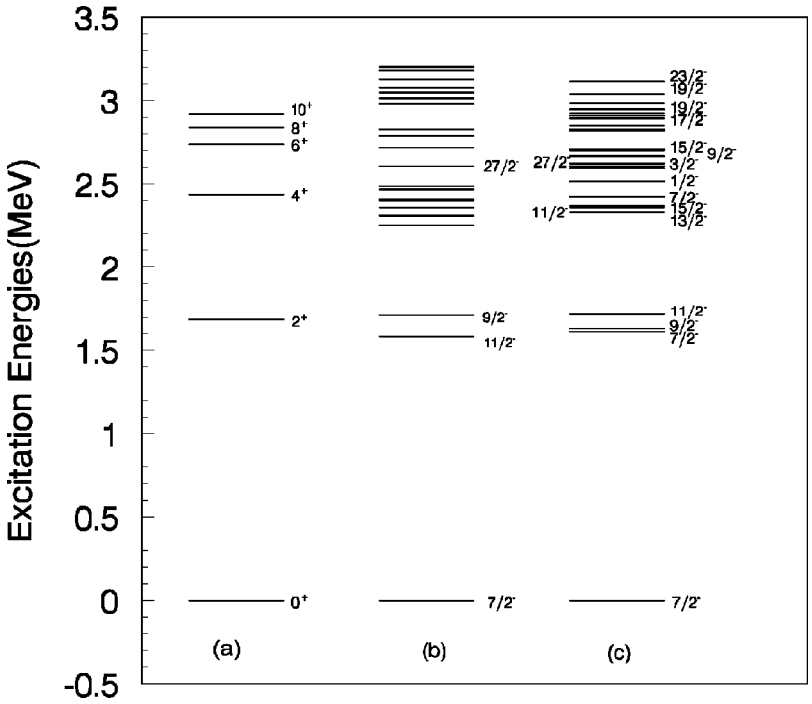

FIG. 6. The homologous structure of the energy levels of $^{149}_{66}\mathrm{Dy}_{83}$ for the negative parity states. The levels of set (a) are parent states, those of set (b) are the experimental results, and those of set (c) are the results of full shell model calculation.

states corresponding to the coupling of an odd proton in the $\pi h_{11/2}$ orbital or an odd neutron in the $\nu f_{7/2}$ orbital to the parent state $\Psi_{J_c}(2N_p,2N_n)$ with an angular momentum J_c. We use this scheme to analyze the full shell model calculations for the nuclei $^{149}_{66}\mathrm{Dy}_{83}$, $^{149}_{65}\mathrm{Tb}_{84}$, $^{151}_{67}\mathrm{Ho}_{84}$, $^{153}_{69}\mathrm{Tm}_{84}$, $^{151}_{68}\mathrm{Er}_{83}$, and $^{151}_{66}\mathrm{Dy}_{85}$ in the following. In order to verify the above idea, we calculate the total one-particle shell model spectroscopic amplitudes defined as

$$S^{J^\pi;T}_{\mathrm{total}}(\rho)=\sum_{k=1}^{N}\,[S^{1/2,J^\pi;T}_k(\rho)]^2$$
$$=\sum_{k=1}^{N}\,[(2J+1)(2T+1)]^{-1}|\langle JT;k|||a^\dagger_\rho|||J_cT_c\rangle|^2 \tag{17}$$

and the corresponding centroid energies defined as

$$E^{J^\pi;T}_{\mathrm{centroid}}=\sum_{k}^{N}\,E^{J^\pi;T}_k[S^{1/2,J^\pi;T}_k]^2/S^{J^\pi;T}_{\mathrm{total}}, \tag{18}$$

where N is the number of final eigenstates with the same J^π and T in the summation. In our calculation $N=10$ can count most of the shell model spectroscopic strengths. $|J_cT_c\rangle$ is the corresponding parent state. The quantities S_{total} and E_{centroid} bear the information of the distribution of the one-particle shell model spectroscopic amplitudes. The quantity E_{centroid} should be located at the position of the corresponding parent state because the S_{total} is most exhausted by the homologous state if the weak coupling scheme holds. Thus the quantities S_{total} and E_{centroid} are very sensitive to the wave functions. The above idea can be also tested by comparing the following $B(E2)$ strength relations between $E2$ transitions $[j\times J_c]_{I_iM_i}\rightarrow[j\times J'_c]_{I_fM_f}$ and $J_c\rightarrow J'_c$. According to the weak coupling scheme, we have the following relation [8]:

$$\frac{B\{E2;(jJ_c)_{I_i}\rightarrow(jJ'_c)_{I_f}\}}{B(E2;J_c\rightarrow J'_c)}=(2I_f+1)(2J_c+1)$$
$$\times W^2(jJ_cI_f2;I_iJ'_c), \tag{19}$$

where W is Racah coefficient defined as in Ref. [8].

$^{149}_{66}\mathrm{Dy}_{83}$ (Fig. 6). The calculated and experimental negative parity levels are compared in Fig. 6. Only a few experimental levels have been assigned. The level density is reproduced in our calculation. According to the calculated results, the levels can be finely interpreted in terms of the configuration scheme that the neutron single-particle state $\nu f_{7/2}$ weakly couples to the independent proton-pair states $\Psi_{J_c}(2,0)$ with $J_c=0^+$, 2^+, 4^+, 6^+, 8^+, and 10^+. The negative parity states ranging from 1.583 to 1.712 MeV are a homologous state family of $\Psi_J(2,0,2,\nu f_{7/2})$ with $J=3/2^-$, $5/2^-$, $7/2^-$, $9/2^-$, and $11/2^-$ (only $11/2^-$ and $9/2^-$ are observed); the states ranging from 2.291 to 2.487 MeV, whose spins and parities (J^π) have not been assigned in experiments, are probably a family of homologous states $\Psi_J(2,0,4,\nu f_{7/2})$ with $J=1/2^-$, $3/2^-$, $5/2^-$, $7/2^-$, $9/2^-$, $11/2^-$, $13/2^-$, and/or $15/2^-$; the states ranging from 2.607 to about 3.0 MeV, whose J^π also have not been assigned in experiments, may be the homologous state family of $\Psi_J(2,0,J_c,\nu f_{7/2})$ with $J_c=6^+$, 8^+, or 10^+. It must be emphasized that not all the homologous states in a family appear because of the configuration mixings, especially for low-spin states. This can be seen in the wave functions listed in Table III. For example, the component of the configuration $\pi h^2_{11/2}\nu f_{7/2}$ are less than 50% in the $3/2^-$ and $5/2^-$ states in the $\Psi_J(2,0,2,\nu f_{7/2})$ family and the other configurations have large contributions. Similar phenomena happen in the low-spin states in other homologous state families and in other nuclei which we will discuss next. We also list the wave functions of these bad homologous states in the table for comparison. The homologous structure can be verified by

TABLE III. The excitation energies, the weights of the main configurations, the one-neutron spectroscopic amplitudes calculated by Eq. (17), and the corresponding centroid energies of homologous state families calculated by Eq. (18) for $^{149}_{66}Dy_{83}$. The homologous states are given rise by coupling the $\nu f_{7/2}$ neutron to the parent states 2^+,6^+,8^+, and 10^+ in $^{148}_{66}Dy_{82}$. The main configurations are listed in percentage. For the parent states the neutron configuration should be ignored. The second column is for the parent states and the following columns are for the homologous state family.

J^π	2^+	$3/2^-$	$3/2^-$	$5/2^-$	$5/2^-$	$7/2^-$	$9/2^-$	$11/2^-$	
E_{cal} (MeV)	1.688	1.798	1.954	1.753	1.898	1.595	1.617	1.705	
$\pi h^2_{11/2}\nu f_{7/2}$	97.64	46.28	42.62	51.96	41.77	96.00	96.84	91.17	
$\pi h^2_{11/2}\nu p_{3/2}$		13.25			3.56				
$\pi h^2_{11/2}\nu f_{5/2}$				36.68	45.92				
$\pi d^2_{3/2}\nu f_{7/2}$		8.80							
$\pi s_{1/2}d_{3/2}\nu f_{7/2}$		30.33	34.51	4.95	3.06				
$S_{total}(\nu f_{7/2})$		0.994	0.994	0.994	0.994	0.980	0.996	0.997	
$E_{centriod}$ (MeV)		1.806	1.806	1.859	1.859	1.585	1.662	1.772	
J^π	4^+	$1/2^-$	$3/2^-$	$5/2^-$	$7/2^-$	$9/2^-$	$11/2^-$	$13/2^-$	$15/2^-$
E_{cal} (MeV)	2.435	2.516	2.595	2.391	2.409	2.421	2.341	2.316	2.367
$\pi h^2_{11/2}\nu f_{7/2}$	100	85.05	83.94	80.38	92.97	66.70	84.58	99.25	97.56
$\pi h^2_{11/2}\nu h_{9/2}$					2.42	30.44	2.19		
$\pi h^2_{11/2}\nu p_{3/2}$		2.83	10.75	8.03					1.29
$\pi h^2_{11/2}\nu f_{5/2}$			1.10	5.29	1.01				
$\pi h^2_{11/2}\nu p_{1/2}$		6.82							
$\pi s_{1/2}d_{3/2}\nu f_{7/2}$							10.89		
$S_{total}(\nu f_{7/2})$	0.996	0.993	0.985	0.985	0.985	0.991	0.996	0.997	
$E_{centriod}$ (MeV)	2.514	2.546	2.438	2.444	3.394	2.324	2.357	2.448	
J^π	6^+	$5/2-$	$7/2^-$	$9/2^-$	$11/2^-$	$13/2^-$	$15/2^-$	$17/2^-$	$19/2^-$
E_{cal} (MeV)	2.739	2.787	2.712	2.662	2.658	2.610	2.692	2.606	2.592
$\pi h^2_{11/2}\nu f_{7/2}$	100	64.56	48.71	81.70	64.09	84.21	97.34	99.31	99.63
$\pi h^2_{11/2}\nu h_{9/2}$		1.74	2.38	1.19	34.67	13.99			
$\pi h^2_{11/2}\nu p_{3/2}$		5.16	18.61	1.54			1.00		1.46
$\pi h^2_{11/2}\nu f_{5/2}$		3.06	1.25	1.14					
$\pi d^2_{3/2}\nu f_{7/2}$		9.76	18.50	4.24					
$\pi s_{1/2}d_{3/2}\nu f_{7/2}$		11.78	2.13	9.98					
$S_{total}(\nu f_{7/2})$		0.950	0.863	0.956	0.980	0.992	0.991	0.996	0.998
$E_{centriod}$ (MeV)		2.778	2.718	2.666	2.686	2.798	2.685	2.634	2.714
J^π	8^+	$9/2^-$	$11/2^-$	$13/2^-$	$15/2^-$	$17/2^-$	$19/2^-$	$21/2^-$	$23/2^-$
E_{cal} (MeV)	2.840	2.837	2.840	2.823	2.803	2.893	2.940	2.692	2.663
$\pi h^2_{11/2}\nu f_{7/2}$	100	92.47	96.49	87.59	96.88	97.19	98.11	98.80	98.31
$\pi h^2_{11/2}\nu f_{5/2}$		2.20	1.06	2.04					
$S_{total}(\nu f_{7/2})$		0.939	0.987	0.989	0.983	0.996	0.999	1.000	1.000
$E_{centriod}$ (MeV)		2.800	2.766	2.811	2.828	2.916	2.886	2.714	2.733
J^π	10^+	$13/2^-$	$15/2^-$	$17/2^-$	$19/2^-$	$21/2^-$	$23/2^-$	$25/2^-$	$27/2^-$
E_{cal} (MeV)	2.920	2.931	2.908	2.970	3.030	2.932	3.110	2.880	2.687
$\pi h^2_{11/2}\nu f_{7/2}$	100	81.74	97.55	97.63	97.69	96.87	98.69	99.08	99.92
$\pi h^2_{11/2}\nu h_{9/2}$		16.80	1.19						
$S_{total}(\nu f_{7/2})$		0.980	0.987	0.986	0.998	1.000	1.000	1.000	1.000
$E_{centriod}$ (MeV)		2.791	2.870	2.960	3.035	2.976	3.051	2.895	2.688

checking the relation of Eq. (19). We investigate the following two sets of decays: $27/2^-\rightarrow 23/2^-\rightarrow 19/2^-\rightarrow 15/2^-\rightarrow 11/2^-$ and $25/2^-\rightarrow 21/2^-\rightarrow 17/2^-\rightarrow 11/2^-\rightarrow 19/2^-$. The decays of their corresponding parent states are $10^+\rightarrow 8^+\rightarrow 6^+\rightarrow 4^+\rightarrow 2^+$ in $^{148}_{66}Dy_{82}$. The results are presented in Table IV. The shell model results are in good agreement with the values given by the weak coupling scheme. The spectrum can thus be quite reasonably reproduced by selecting the main configurations according to this weak coupling picture. The calculated one-neutron shell model spectroscopic amplitudes and the corresponding centroid energies further verify the homologous structure of the spectrum. The total one-

TABLE IV. Comparison of the results of $E2$ transitions calculated by the full shell model (SM) and by the weak coupling scheme (WC) [Eq. (19)] for the nucleus $^{149}_{66}\mathrm{Dy}_{83}$.

	WC	SM		WC	SM
$\frac{B(E2;27/2^-\rightarrow 23/2^-)}{B(E2;10^+\rightarrow 8^+)}$	1.000	1.267	$\frac{B(E2;25/2^-\rightarrow 21/2^-)}{B(E2;10^+\rightarrow 8^+)}$	0.939	0.710
$\frac{B(E2;23/2^-\rightarrow 19/2^-)}{B(E2;8^+\rightarrow 6^+)}$	1.000	1.099	$\frac{B(E2;21/2^-\rightarrow 17/2^-)}{B(E2;8^+\rightarrow 6^+)}$	0.907	0.923
$\frac{B(E2;19/2^-\rightarrow 15/2^-)}{B(E2;6^+\rightarrow 4^+)}$	1.000	1.011	$\frac{B(E2;17/2^-\rightarrow 13/2^-)}{B(E2;6^+\rightarrow 4^+)}$	0.844	0.874
$\frac{B(E2;15/2^-\rightarrow 11/2^-)}{B(E2;4^+\rightarrow 2^+)}$	1.000	1.121	$\frac{B(E2;13/2^-\rightarrow 9/2^-)}{B(E2;4^+\rightarrow 2^+)}$	0.681	0.681

neutron shell model spectroscopic amplitudes $S(\nu f_{7/2})_{\mathrm{total}}$ and the corresponding centroid energies calculated by Eq. (18) for the different homologous state families are also presented in Table III in the last two lines. The centroid energies are located at the positions of the corresponding parent states quite well. This also happens for the bad homologous states because the $[S^{1/2}(\nu f_{7/2})]^2$ is distributed in two energy-near states which have a similar weight of component $\pi h_{11/2}^2 \nu f_{7/2}$ as shown for the above mentioned $3/2^-$ and $5/2^-$ states in the second line of the table. In a word, the spectrum of $^{149}_{66}\mathrm{Dy}_{83}$ can be reasonably interpreted by the homologous state concept. There are several single-particle excited states which are not displayed in Fig. 6 and Table III. They can also be explained as homologous states by weakly coupling the corresponding single-particle states to the ground state (0^+) of the parent nucleus. The first excited state $3/2^-$ can be interpreted as the homologous state $\Psi_{3/2}(2,0,\nu p_{3/2})$. Its excitation energy is 1.03 MeV, just a little bit smaller than that in $^{147}_{64}\mathrm{Gd}_{83}$ (1.13 MeV). The second excited state $9/2^-$ is a neutron $h_{9/2}$ state and can be regarded as a homologous state $\Psi_{9/2}(2,0,0,\nu h_{9/2})$. The strong proton-neutron interactions for $\pi h_{11/2}-\nu h_{9/2}$ reduce the energy of this excited state from 1.40 MeV in the $^{147}_{64}\mathrm{Gd}_{83}$ to 1.09 MeV in $^{149}_{66}\mathrm{Dy}_{83}$. Because of the high excited energies of the neutron single-particle orbitals $p_{1/2}$ and $f_{5/2}$, the single-particle excitations for these two states are strongly mixed with other configurations. As to the positive parity states, only a few have been assigned in experiments. According to our calculation, the $21/2^+$ state at 2.55 MeV, which is a stretch state in our model space, can be considered to be a homologous state to the parent state 7^- (2.75 MeV) in $^{148}_{66}\mathrm{Dy}_{82}$; the $17/2^+$ state at 2.251 MeV is a homologous state to the parent state 5^-. For the other positive parity states, the two main configurations $\pi s_{1/2} h_{11/2} \nu f_{7/2}$ and $\pi d_{3/2} h_{11/2} \nu f_{7/2}$ mix strongly because of their approximate average energies $\langle H \rangle$ and, therefore, these states are much less similar to the corresponding negative parity states in $^{148}_{66}\mathrm{Dy}_{82}$, which are given rise from the configuration $\pi s_{1/2} h_{11/2}$ or $\pi d_{3/2} h_{11/2}$.

$^{149}_{65}\mathrm{Tb}_{84}$ (Fig. 7). The structure of this nucleus was investigated by Lach *et al.* [19] using an empirical shell model. In

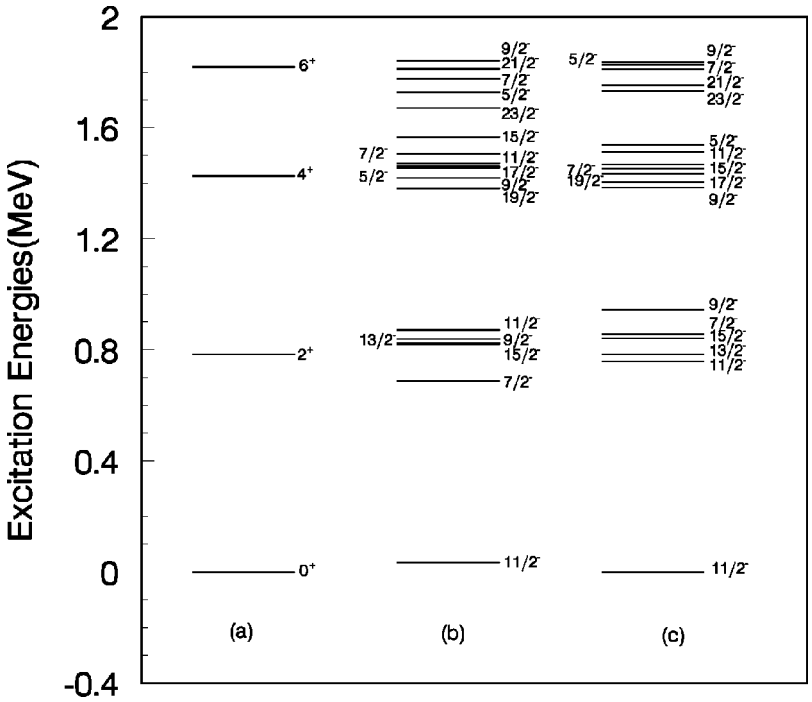

FIG. 7. The homologous structure of the energy levels of $^{149}_{65}\mathrm{Tb}_{84}$ for the negative parity states. The levels of set (a) are parent states, those of set (b) are the experimental results, and those of set (c) are the results of full shell model calculation.

TABLE V. The excitation energies, the main configurations, the one-proton spectroscopic amplitudes [calculated by Eq. (17)], and the corresponding centroid energies [calculated by Eq. (18)] of the homologous state families in $^{149}_{65}Tb_{84}$ which are given rise from coupling the $h_{11/2}$ proton to the parent states 2^+, 4^+, and 6^+ in $^{148}_{64}Gd_{84}$.

J^π	2^+	$7/2^-$	$9/2^-$	$11/2^-$	$13/2^-$	$15/2^-$				
E_{cal} (MeV)	0.812	0.859	0.945	0.759	0.785	0.842				
$\nu f^2_{7/2}\pi h_{11/2}$	98.49	91.54	97.06	97.57	98.51	95.47				
$\nu h^2_{9/2}\pi h_{11/2}$				2.89						
$\nu f^2_{5/2}\pi h_{11/2}$				1.72						
$\nu f_{7/2}p_{3/2}\pi h_{11/2}$		5.06				2.66				
$\nu p_{3/2}\pi h_{11/2}$				2.57						
$S_{total}(\pi h_{11/2})$			0.993	0.994	0.995	0.997				
$E_{centroid}$ (MeV)			0.961	0.745	0.817	0.892				
J^π	4^+	$3/2^-$	$5/2^-$	$7/2^-$	$9/2^-$	$11/2^-$	$13/2^-$	$15/2^-$	$17/2^-$	$19/2^-$
E_{cal} (MeV)	1.475	1.451	1.539	1.469	1.385	1.516	1.598	1.453	1.404	1.434
$\nu f^2_{7/2}\pi h_{11/2}$	99.12	87.24	83.64	94.34	93.47	94.90	97.27	96.19	97.88	96.59
$\nu f_{7/2}h_{9/2}\pi h_{11/2}$			10.65	1.81	2.10	2.17				
$\nu f_{7/2}f_{5/2}\pi h_{11/2}$		3.88	3.48	1.60	1.12					
$\nu f_{7/2}p_{3/2}\pi h_{11/2}$		2.48		1.22	1.96	1.08		1.44		
$\nu f_{7/2}p_{1/2}\pi h_{11/2}$		3.39								
$S_{total}(\nu h_{11/2})$		0.992	0.992	0.977	0.975	0.991	0.984	0.991	0.997	0.998
$E_{centriod}$ (MeV)		1.551	1.620	1.489	1.425	1.545	1.584	1.462	1.434	1.496
J^π	6^+	$1/2^-$	$3/2^-$	$5/2^-$	$7/2^-$	$9/2^-$	$11/2^-$	$13/2^-$	$15/2^-$	$17/2^-$
E_{cal} (MeV)	1.872	1.734	1.799	1.828	1.762	1.837	1.917	1.934	1.938	1.934
$\nu f^2_{7/2}\pi h_{11/2}$	98.40	81.60	89.80	91.29	79.94	89.97	86.80	87.53	84.64	90.78
$\nu f_{7/2}h_{9/2}\pi h_{11/2}$		17.41	1.88	5.60	22.34	3.73	1.65		1.35	
$\nu f_{7/2}f_{5/2}\pi h_{11/2}$			7.34	1.11		2.51	3.33	3.35	2.58	2.24
$\nu f_{7/2}p_{3/2}\pi h_{11/2}$				1.43	1.46	1.88	6.01	6.48	9.90	3.53
$S_{total}(\pi h_{11/2})$		1.000	0.992	0.986	0.977	0.965	0.957	0.967	0.973	0.975
$E_{centroid}$ (MeV)		1.848	1.835	1.826	1.829	1.859	1.921	1.973	1.961	1.966
J^π	6^+	$19/2^-$	$21/2^-$	$23/2^-$						
E_{cal} (MeV)	1.872	2.061	1.754	1.733						
$\nu f^2_{7/2}\pi h_{11/2}$	98.84	97.10	93.68	96.80						
$\nu f_{7/2}h_{9/2}\pi h_{11/2}$				2.27						
$\nu f_{7/2}f_{5/2}\pi h_{11/2}$		1.69								
$\nu f_{7/2}p_{3/2}\pi h_{11/2}$			3.83							
$S_{total}(\pi h_{11/2})$		0.998	1.000	1.000						
$E_{centroid}$ (MeV)		2.022	1.812	1.738						

our calculation, the homologous structure is also obvious in the negative parity spectrum and clearly displayed in Fig. 7. This homologous structure is even better than that in the spectrum of $^{149}_{66}Dy_{83}$ because of the proton intruder single-particle state $\pi h_{11/2}$. The low-lying state $11/2^-$ is a quite good proton $\pi h_{11/2}$ single-particle state as in $^{147}_{65}Tb_{82}$, i.e., a good homologous state $\Psi_{11/2}(0,2,0,\nu h_{11/2})$. The negative parity states $7/2^-$, $9/2^-$, $11/2^-$, and $15/2^-$ ranging from 0.69 to 0.9 MeV are well located at the positions of the homologous states $\Psi_J(0,2,2,\pi h_{11/2})$ with $J=7/2^-$, $9/2^-$, $11/2^-$, and $15/2^-$. The other negative parity states below 2.0 MeV have a similar structure. The states ranging from 1.382 to about 1.58MeV and from about 1.65 to 1.85 MeV could be homologous states $\Psi_J(0,2,J_c,\pi h_{11/2})$ with $J_c=4^+$ and 6^+, respectively. The calculated wave functions and one-proton shell model spectroscopic amplitudes $[S^{1/2}(\pi h_{11/2})]^2$ for different homologous state families are listed in Table V. We see again that all the centroid energies are located at the positions of the corresponding parent states even for the bad homologous states because of the same reasons as in $^{149}_{66}Dy_{83}$. For the positive parity states, similar results are obtained as in $^{149}_{66}Dy_{83}$, i.e., the stretch states are good homologous states and the other states have strong configuration mixings. Therefore, the intruder proton single-particle state $\pi h_{11/2}$ plays an essential role for the homologous structure of the negative parity states in $^{149}_{66}Dy_{83}$ and $^{149}_{65}Tb_{84}$ as

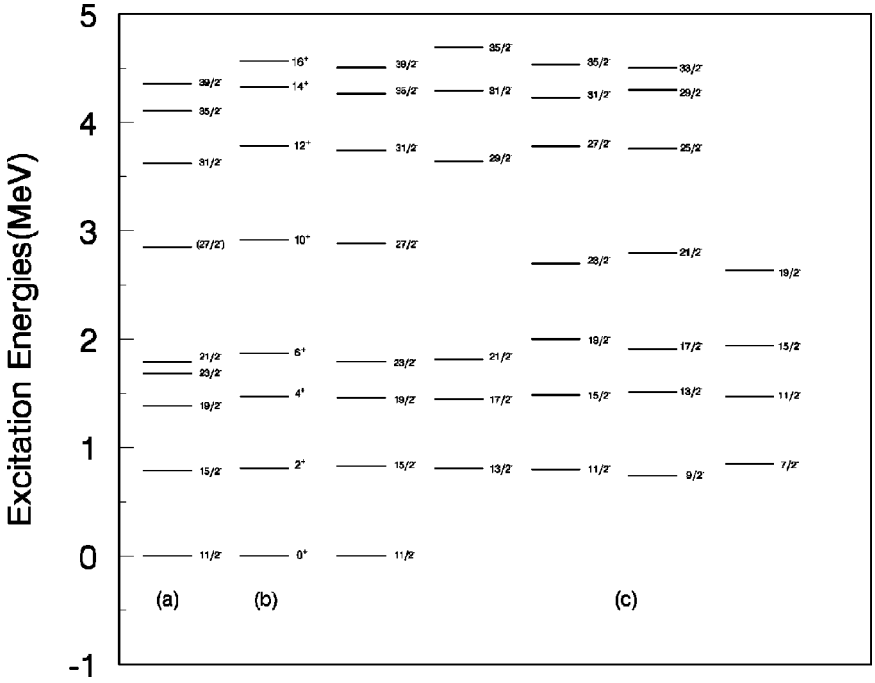

FIG. 8. The homologous structure of the energy levels of $^{151}_{67}Ho_{84}$ for the negative parity states. The levels of set (a) are the experimental results, those of set (b) are the parent states, and those set of (c) are the results of full shell model calculation (see the text for a detailed explanation).

well as in the nuclei $^{151}_{67}Ho_{84}$, etc., discussed below. This is one of the reasons why the simple shell model calculation can reproduce the negative parity states, especially the high-spin states quite well.

$^{151}_{67}Ho_{84}$ (Fig. 8). The high-spin states of this nucleus were studied first by Gizon *et al.* [20], and then by Zhang *et al.* [7] both using in beam method. They found that the energy levels of the yrast high-spin states could be reproduced with very high accuracy using the configurations $\pi h^3_{11/2}\nu f^2_{7/2}$ and $\pi h^3_{11/2}\nu h_{9/2}f_{7/2}$. We have carried out a calculation in a full $N=82-126$ major shell. Just like the results in Ref. [7], the high-spin states are reproduced quite well in our full shell model calculation. The homologous structure is obvious in these states, which is clearly displayed in Fig. 8. The level structures from the ground state $11/2^-$ to $23/2^-$, and from the second $27/2^-$ to $39/2^-$ are very similar to each other and are homologous to their parent states $\Psi_{J_c}(2,2)$ with $J_c=0^+, 2^+, 4^+, 6^+, 10^+, 12^+, 14^+, 16^+$. The weights of the dominant configuration $\pi h^3_{11/2}\nu f^2_{7/2}$ for $15/2^-$, $19/2^-$, $21/2^-$, and $23/2^-$ are 76.81, 78.62, 78.38, and 78.21 %, very close to the weights 81.19, 82.69, and 81.62 % for the dominant configuration $\pi h^2_{11/2}\nu f^2_{7/2}$ in the parent states 2^+, 4^+, and 6^+ in $^{150}_{66}Dy_{84}$. Much purer homologous wave functions for the states $27/2^-$, $31/2^-$, $35/2^-$, and $39/2^-$ to the parent states $\Psi_{J_c}(2,2)$ with $J_c=10^+$, 12^+, 14^+, and 16^+ in the $^{150}_{66}Dy_{84}$ are obtained. Thus these states can be well interpreted as an odd proton weakly coupled to the excited states of the independent nucleon pair in the $^{150}_{66}Dy_{84}$. Our calculation also successfully reproduces the high-spin states arose from the configuration $\pi h^3\nu f_{7/2}h_{9/2}$. These states can be understood

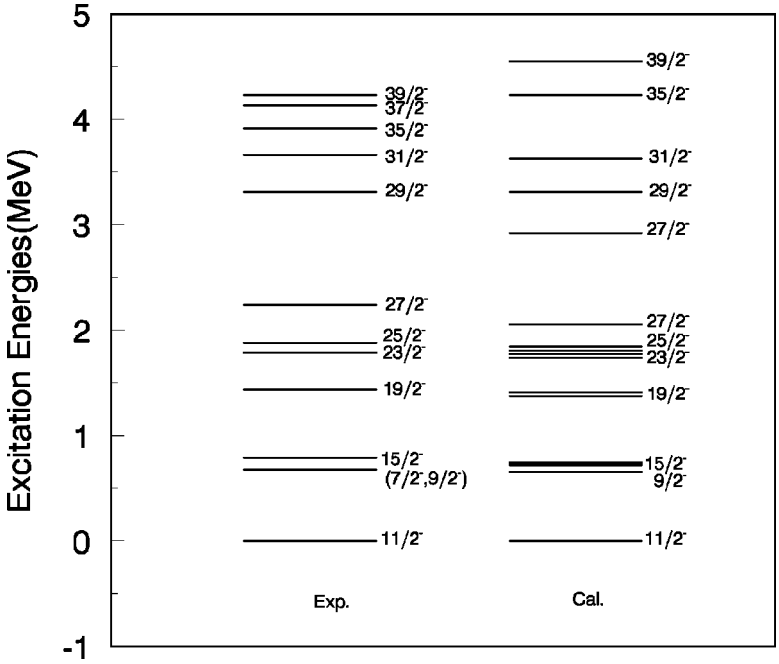

FIG. 9. Theoretical and experimental energy levels of $^{153}_{69}Tm_{84}$ for the negative parity states.

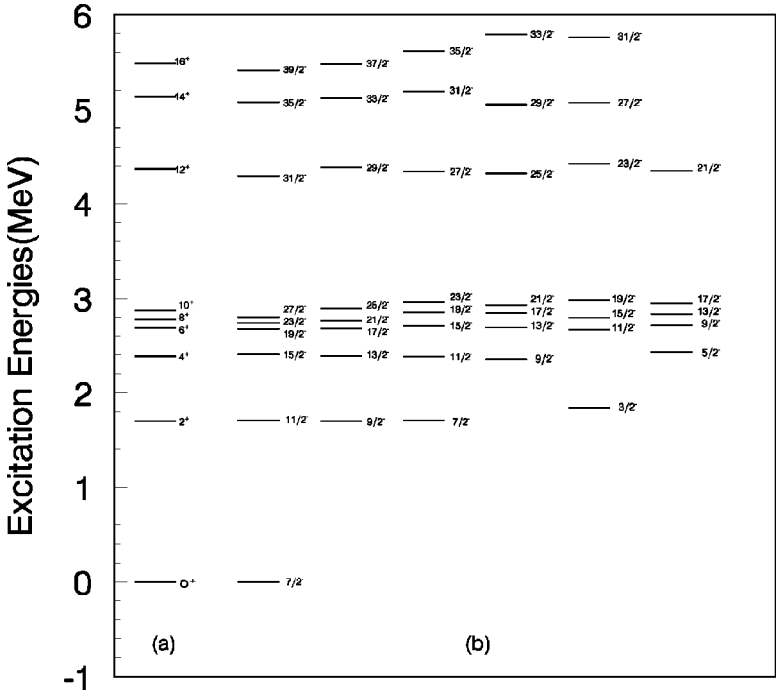

FIG. 10. The theoretical prediction of the homologous states of $^{151}_{68}\mathrm{Er}_{83}$. The levels of set (a) are the parent states and those of set (b) are the results of full shell model calculation (see the text for a detailed explanation).

by a bit stronger coupling of the odd $\pi h_{11/2}$ proton to the states with the characteristic configuration $(\pi h^2_{11/2})_{0^+} \otimes (\nu f_{7/2} h_{9/2})_{6^+ \text{ or } 8^+}$ in the $^{150}_{66}\mathrm{Dy}_{84}$.

$^{153}_{69}\mathrm{Tm}_{84}$ (Fig. 9). It is interesting to note again that the spectrum of $^{153}_{69}\mathrm{Tm}_{84}$ is almost identical to that of $^{151}_{67}\mathrm{Ho}_{84}$. This is not surprising because the spectrum of $^{153}_{69}\mathrm{Tm}_{84}$ is an excellent homologous state family of its parent spectrum of $^{152}_{68}\mathrm{Er}_{84}$.

$^{151}_{68}\mathrm{Er}_{83}$ (Fig. 10). The negative parity levels of $^{151}_{68}\mathrm{Er}_{83}$ are expected to be classified by using the above homologous state concept. The predicted levels are presented in Fig. 10 and show a clear homologous structure to the parent states of the $^{150}_{68}\mathrm{Er}_{82}$, which can be explained by the weak coupling of the odd valence neutron in $\nu f_{7/2}$ orbital to two independent proton pairs. The wave functions given in Table VI also clearly show the homologous structure, especially for the high-spin states. This homologous structure is also confirmed by the calculated one-neutron shell model spectroscopic amplitudes which are similar to the results in $^{149}_{66}\mathrm{Dy}_{83}$ and $^{149}_{65}\mathrm{Tb}_{84}$. However, the available experimental data of these levels are not sufficient to show such a structure. More experiments should be done to test the predicted results.

$^{151}_{66}\mathrm{Dy}_{85}$ (Fig. 11). The concept of homologous states is no longer valid for the levels of $^{151}_{66}\mathrm{Dy}_{85}$. The large possibility of exciting neutrons from the $f_{7/2}$ orbital to the $h_{9/2}$ as well as other orbitals in the low-lying states breaks the validity of the independent neutron pair motion and destroys the corresponding homologous structure. It is impossible to reproduce the experimental data using simple configurations.

IV. DISCUSSIONS AND CONCLUSIONS

The calculated results for the nuclei in $A \sim 150$ mass region clearly show the independent nucleon pair motion which implies that the proton pairs in $\pi 1h_{11/2}$, $\pi 2d_{3/2}$, and $\pi 3s_{1/2}$ orbitals and the neutron pair in $\nu f_{7/2}$ orbital are moving almost independently because of the weak interactions among them. The states which are given rise from the weak coupling of an odd nucleon to the excitation states of independent nucleon pairs share homologous structures to their parent states. These are the reasons that the simple shell model calculations are surprisingly successful for these nuclei. One should expect that the concept of homologous states, which is an outcome of the weak coupling of an odd nucleon to the corresponding parent state, is a useful tool to analyze the spectra of heavy nuclei where a few nucleons or nucleon pairs are at the beginning of a major shell or subshell if the residual interactions are much smaller than the single-particle energies (i.e., the mean field). This can be confirmed by one of our recent investigations of the high excited states of ^{206}Pb induced by the reaction $^{209}\mathrm{Bi}(\vec{p},\alpha)^{206}\mathrm{Pb}$ [12]. These states can be described in the terms of one proton in $h_{9/2}$ single-particle state weakly coupled to the low lying states in ^{205}Tl so that the level structure and wave functions of these high excited states in ^{206}Pb are very similar to those of the low-lying states in ^{205}Tl. This similarity is called homology.

There are three factors which give rise to the independent pair approximation and the homologous structure in nuclei in $A \sim 150$ mass region. First, the high angular momentum intruder proton single-particle state $\pi h_{11/2}$ plays an essential role. Its pair energy is much larger than those of $\pi d_{3/2}$ and $\pi s_{1/2}$. The excited states, especially the high-spin states, of the proton configuration $\pi h^z_{11/2}$ are isolated from the other states due to the parity and angular momentum conservations. This makes the independent pair approximation very effective for the nuclei with $Z=64+z$ and $N=82$. Secondly, the weak proton-neutron interaction for $\pi h_{11/2} - \nu f_{7/2}$ also keeps this approximation valid to the nuclei having both valence protons and neutrons. The last factor is the large energy gaps between the neutron orbitals $\nu f_{7/2}$ and the others in $^{147}_{64}\mathrm{Gd}_{83}$. This makes other single-particle states have little

TABLE VI. The excitation energies, the main configurations of the predicted homologous state families in the $^{151}_{68}Er_{83}$, which are given rise from the coupling of the $\nu f_{7/2}$ neutron to the parent states 2^+, 4^+, 6^+, 8^+, 10^+, 12^+, 14^+, and 16^+ in $^{150}_{68}Er_{82}$. The other notations have the same meanings as those in Table III.

J^π	2^+	$11/2^-$	$9/2^-$	$7/2^-$	$5/2^-$	$3/2^-$			
E_{cal} (MeV)	1.707	1.710	1.705	1.709	1.888	1.845			
$\pi h^4_{11/2}\nu f_{7/2}$	89.35	73.46	83.37	78.07	41.34	73.19			
J^π	4^+	$15/2^-$	$13/2^-$	$11/2^-$	$9/2^-$	$7/2^-$	$5/2^-$		
E_{cal} (MeV)	2.388	2.407	2.392	2.385	2.353	2.451	2.431		
$\pi h^4_{11/2}\nu f_{7/2}$	92.39	86.86	86.81	84.27	75.31	58.73	77.59		
J^π	6^+	$19/2^-$	$17/2^-$	$15/2^-$	$13/2^-$	$11/2^-$	$9/2^-$		
E_{cal} (MeV)	2.690	2.675	2.679	2.705	2.693	2.666	2.712		
$\pi h^4_{11/2}\nu f_{7/2}$	92.45	86.41	86.69	87.65	86.10	84.32	75.47		
J^π	8^+	$23/2^-$	$21/2^-$	$19/2^-$	$17/2^-$	$15/2^-$	$13/2^-$	$11/2^-$	$9/2^-$
E_{cal} (MeV)	2.780	2.741	2.760	2.858	2.850	2.793	2.835	2.947	2.823
$\pi h^4_{11/2}\nu f_{7/2}$	92.47	86.59	86.60	89.23	88.12	86.85	80.47	83.47	81.45
J^π	10^+	$27/2^-$	$25/2^-$	$23/2^-$	$21/2^-$	$19/2^-$	$17/2^-$	$15/2^-$	$13/2^-$
E_{cal} (MeV)	2.879	2.804	2.896	2.963	2.930	2.983	2.947	2.923	2.909
$\pi h^4_{11/2}\nu f_{7/2}$	92.42	86.36	87.60	89.55	87.00	87.12	87.04	84.55	80.26
J^π	12^+	$31/2^-$	$29/2^-$	$27/2^-$	$25/2^-$	$23/2^-$			
E_{cal} (MeV)	4.371	4.299	4.391	4.347	4.324	4.246			
$\pi h^4_{11/2}\nu f_{7/2}$	97.371	85.53	95.45	89.87	84.31	83.93			
J^π	14^+	$35/2^-$	$33/2^-$	$31/2^-$	$29/2^-$	$27/2^-$			
E_{cal} (MeV)	5.133	5.072	5.119	5.188	5.048	5.070			
$\pi h^4_{11/2}\nu f_{7/2}$	100	98.86	99.80	96.44	98.00	95.12			
J^π	16^+	$39/2^-$	$37/2^-$	$35/2^-$	$33/2^-$	$31/2^-$			
E_{cal} (MeV)	5.490	5.412	5.482	5.616	5.794	5.763			
$\pi h^4_{11/2}\nu f_{7/2}$	100	99.38	98.85	97.91	95.78	95.22			

influence on the configuration $\pi h^z_{11/2}\nu f^n_{7/2}$. However, this energy gap effect will reduce as neutron number increases beyond $N=84$ as has been shown in the spectra of $^{151,152}_{66}Dy_{85,86}$. Strong configuration mixings due to the excitation of valence neutrons into other orbitals make the independent pair approximation invalid and destroys the corresponding homologous structure, as has been shown in nuclei $^{151,152}_{66}Dy_{85,86}$.

The independent pair approximation provides a natural explanation to the identification of the spectra of $^{150}_{66}Dy_{84}$ and $^{152}_{68}Er_{84}$ as well as $^{151}_{67}Ho_{84}$ and $^{153}_{69}Tm_{84}$. Further experiments are expected to test the prediction of the new mode, i.e., the phenomenon of independent pair motion in these nuclei.

It must be pointed out that the effect of the broken subshell $Z=64$ is totally ignored in this paper. The energy gap of this subshell is about 2.5 MeV, and the protons below the $Z=64$ shell can be scattered into the shell above $Z=64$. This leads to particle-hole (p-h) excitations. This effect can be fully taken into account by extending the proton model space from the 64–82 subshell to the 50–82 full major shell. The difficulty for this extension comes from two aspects: (i) the calculation is very complicated and (ii) there is an ambiguity in residual interactions. Here we just discuss the effect from one-particle one-hole ($1p$-$1h$) excitations in a qualitative way. The $1p$-$1h$ excitations may have important effects on the negative parity states of the even-even nuclei and the positive parity states of the even-odd nuclei, especially on the low-spin states because of the parity and angular momentum restrictions. For the negative parity states of even-odd nuclei, such as $^{149}_{65}Tb_{84}$, etc., a proton excited from the below $Z=64$ subshell can only fill in the $\pi s_{1/2}$ or $\pi d_{3/2}$ orbital due to the parity restriction. However, the influence is reduced due to the fact that the average proton particle-hole interactions of $V_p(g^{-1}_{7/2}-d^1_{3/2}$ or $s^1_{1/2})$ and $V_p(d^{-1}_{5/2}-d^1_{3/2}$ or $s^1_{1/2})$ across the $Z=64$ subshell are smaller than the average proton hole-hole interactions $\overline{V}_p(d^{-2}_{5/2})$ and $\overline{V}_p(g^{-2}_{7/2})$. For the

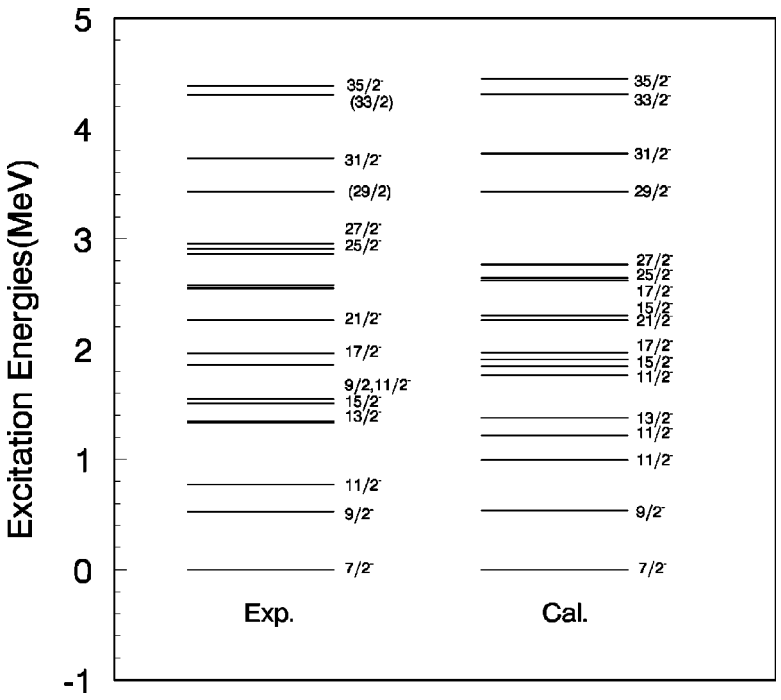

FIG. 11. Theoretical and experimental energy levels of $^{151}_{66}\mathrm{Dy}_{85}$ for the negative parity states.

high-spin states, the $1p$-$1h$ excitations can only provide at most five units of angular momenta (the $\pi g^{-1}_{7/2} - \pi d^{1}_{3/2}$ excitation) and have a small impact on the levels discussed in this paper because of the angular momentum restriction. Moreover, the most important thing is that the effect of particle-hole excitations will not change the weak coupling scheme for the nuclei studied in the paper. Therefore, the physical pictures of the independent nucleon-pair motion and the homologous state structure are still valid as the shell model space is extended.

As a whole, our full shell model calculations give a good overall description of the nuclei studied. The positive parity states up to 10^+ in $^{148}_{66}\mathrm{Dy}_{82}$ and up to 6^+ in $^{148}_{64}\mathrm{Gd}_{84}$ can be understood as proton pair excitations in $\pi h_{11/2}$ and neutron pair excitations in $\nu f_{7/2}$, respectively. The spectra of $^{150}_{66}\mathrm{Dy}_{84}$ and $^{150,152}_{68}\mathrm{Er}_{82,84}$ can be interpreted as independent pair excitations and share a similar level structure. The level structures of $^{149}_{66}\mathrm{Dy}_{83}$, $^{149}_{65}\mathrm{Tb}_{84}$, $^{151}_{67}\mathrm{Ho}_{84}$, and $^{153}_{69}\mathrm{Tm}_{84}$ can be explained using the concept of homologous states which are given rise from the weak coupling of an odd nucleon to the parent states of independent nucleon pair excitations. The predicted levels of $^{151}_{68}\mathrm{Er}_{83}$ show a clear homologous structure to its parent states of $^{150}_{68}\mathrm{Er}_{82}$. Experiments on this nucleus are desired to test our predictions. The independent nucleon-pair motion and the corresponding homologous state structure are broken down in $^{151,152}_{66}\mathrm{Dy}_{85,86}$ since the conditions for them to occur are not satisfied and the shell model space is too small to describe them.

ACKNOWLEDGMENTS

This work was supported in part by the National Natural Science Foundation and the Doctoral Education Fund of the State Education Commission of China, and by the Nuclear Industrial Research Fund of China.

[1] P. Kleinheiz, R. Broda, P. J. Daly, S. Lunardi, M. Ogawa, and J. Blomgvist, Z. Phys. A **290**, 279 (1979).

[2] K. S. Toth, Y. A. Ellis-Akovali, F. T. Avignone III, R. S. Moore, D. M. Moltz, J. M. Nitschke, P. A. Wilmarth, P. K. Lemmertz, D. C. Sousa, and A. L. Goodman, Phys. Rev. C **32**, 342 (1985).

[3] P. Kleinheiz, Shell Model and Nuclear Structure; Where Do We Stand? 2nd International Spring Seminary on Nuclear Physics 1988, edited by A. Covello (unpublished).

[4] J. Wilson S. R. Faber, P. J. Daly, I. Ahmad, J. Borggreen, P. Chowdhury, T. L. Khoo, R. D. Lawson, R. K. Smither, and J. Blomqvist, Z. Phys. A **296**, 185 (1980).

[5] R. D. Lawson, Z. Phys. A **303**, 51 (1981).

[6] D. Horn, I. S. Towner, O. Häusser, D. Ward, H. R. Andrews, M. A. Lone, J. F. Sharpey-Schafer, N. Rud, and P. Taras, Nucl. Phys. **A441**, 344 (1985).

[7] C. T. Zhang, P. Kleinheinz, M. Piiparinen, R. Broda, R. Collatz, P. J. Daly, K. H. Maier, R. Menegazzo, G. Sletten, J. Styczen, and J. Blomqvist, Phys. Rev. C **54**, R1 (1996); Z. Phys. A **348**, 65 (1997).

[8] R. D. Lawson, *Theory of the Nuclear Shell Model* (Clarendon, Oxford, 1980).

[9] P. Grabmayr, Prog. Part. Nucl. Phys. **29**, 221 (1992), and references therein.

[10] P. Guazzoni, M. Jaskola, L. Zetta, G. Graw, R. Hertenberger, D. Hofer, P. Schiemenz, V. Atzrott, R. Neu, and G. Staudt, Phys. Rev. C **49**, 2784 (1994); Z. Phys. A **356**, 381 (1997).

[11] E. Gadioli, P. Guazzoni, M. Jaskola, L. Zetta, G. Colombo, G.

Graw, R. Hertenberger, D. Hofer, H. Kader, P. Schiemenz, R. Neu, and G. Staudt, Phys. Rev. C **47**, 1129 (1993); **43**, 2572 (1991).

[12] J. N. Gu, A. Vitturi, C. H. Zhang, P. Guazzoni, L. Zetta, G. Graw, M. Jaskola, and G. Staudt, Phys. Rev. C **55**, 2395 (1997).

[13] B. A. Brown, A. Etchegoyen, and W. D. M. Rae, Computer code OXBASH, MSU-NSCL Report No. 524, 1984 (unpublished).

[14] Nuclear Data sheet, electronic version, URL http://www.nndc.bnl.gov

[15] T. Komppa, R. Komu, M. Kortelahti, J. Muhonen, A. Pakkanen, M. Piiparinen, I. Prochazka, and J. Blomqvist, Z. Phys. A **314**, 314 (1983).

[16] J. Schiffer and W. W. True, Rev. Mod. Phys. **48**, 191 (1976).

[17] Chang-hua Zhang, Jin-nan Gu, and Shun-jin Wang (unpublished).

[18] A. L. Fetter and J. D. Walecka, *Quantum Theory of Many-Particle System* (McGraw-Hill, New York, 1971).

[19] M. Lach, P. Kleinheinz, M. Piiparinen, M. Ogawa, S. Lunardi, M. C. Bosca, J. Styczen, and J. Blomgvist, Z. Phys. A **341**, 25 (1991).

[20] J. Gizon, A. Gizon, S. Andre, J. Genevey, J. Jastrzebski, R. Kossakowski, M. Moszynski, and Z. Preibisz, Z. Phys. A **301**, 67 (1981).